PANDORA Project:
Charged Particle Decay from the IVGDR in ^{27}Al

Atsushi Tami

RCNP, The University of Osaka, Japan

Yohei Sasagawa

Department of Physics, The University of Osaka, Japan

and the PANDORA Collaboration

PANDORA

Photo-Absorption of Nuclei and Decay Observation for Reactions in Astrophysics

10th Workshop on Nuclear Level Density and Gamma Strength,

Oslo, May 18-22, 2026

7th Workshop on Nuclear Level Density and Gamma Strength

Oslo, May 27 - 31, 2019

agreement of the new project: PANDORA

Outline

- PANDORA: Photo-Nuclear Reaction of Light Nuclei
- Intergalactic Propagation of Ultra-High-Energy Cosmic Rays
- Experimental Methods
- ^{27}Al photoabsorption and charged particle decay

Photonuclear Reaction of Light Nuclei

Photo-nuclear Reaction / Excitation of IV GDR

Oscillating electric field induced by an incident photon

→ excites the Iso-Vector Giant Dipole Resonance (IVGDR)

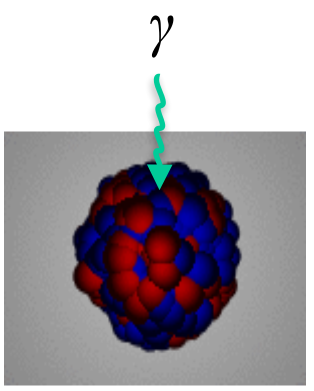

IVGDR

Photo-absorption cross section: dominated by electric dipole (*E1*) excitation

$$\sigma_{\rm abs} \simeq \sigma_{\rm abs}^{E1} = \frac{16\pi^3}{9}\alpha E_\gamma \frac{dB(E1)}{dE_\gamma}$$

$\sigma_{\rm abs}$: photo-absorption cross section

$B(E1)$: electric-dipole reduced transition probability

E_γ : photon-energy = nuclear excitation energy

α : fine structure constant

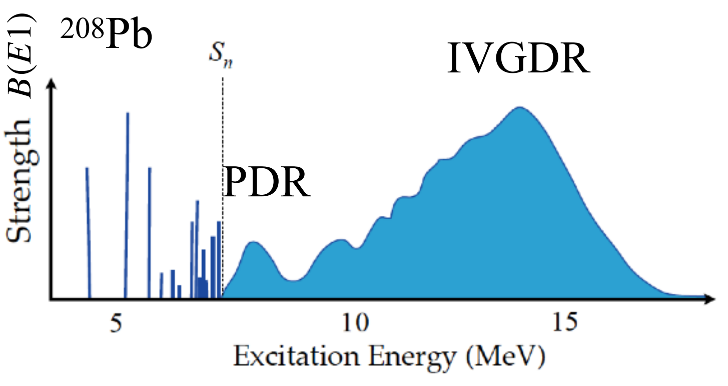

Stable light nuclei, E1 response

Fundamental ⇔ Exotic

Photo-nuclear Reactions: Light Nuclei

For light nuclei

- photo-abs. c.s. $\neq$ (γ,xn) c.s.

large branch to *p* similar to *n* and sizable α emissions

lack of data, especially for charged particle decays

- Challenges to theoretical models

structure (photo-absorption) + reaction (decay)

Structure

- stronger shell effect
- nuclear deformation
- nucleon correlations:

  α clustering, *np* pairing, tensor correlation,…

Decay

- direct and pre-equilibrium decay process in addition to statistical decays
- isospin selection rule in the α-decay process

^{13}C(γ,n)

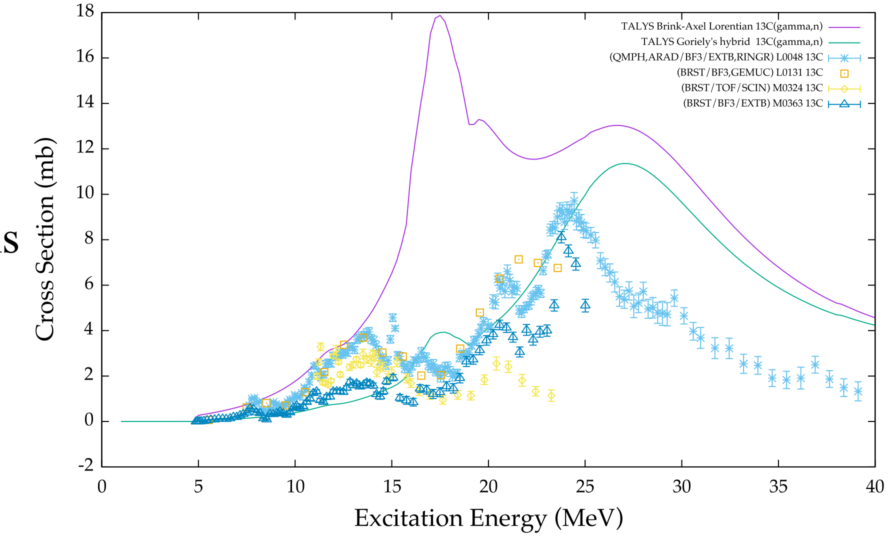

Example: ^{13}C(γ,xn) reaction data and predictions (TALYS)

- Big inconsistency among experimental data
- Unsatisfactory theoretical predications

^{28}Si(γ,abs) Ahrens et al.

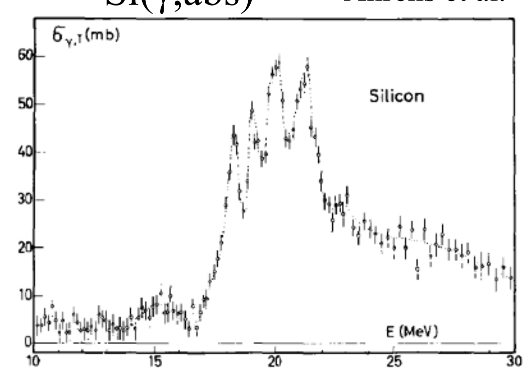

Systematic Measurement on Photo-Absorption Cross Section and decays for light stable nuclei for

- E1 excitation strength distribution
- n, p, α, γ decay branching ratios
- 10-20 light stable nuclei: A<60

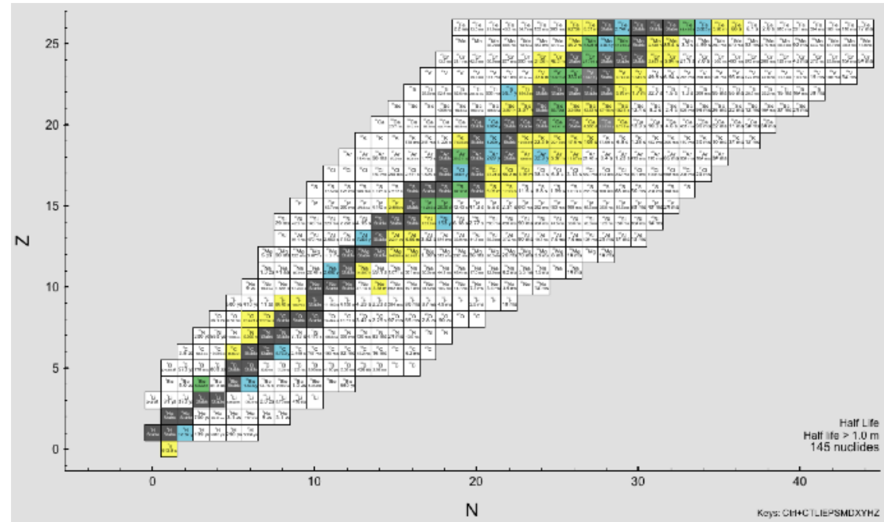

PANDORA Project:

PANDORA

Photo-Absorption of Nuclei and Decay Observation for Reactions in Astrophysics

- Systematic measurement

- Reference target: ^{27}Al (and ^{12}C)

- Consistency check and complementary information by using virtual and real photon measurements

RCNP

iThemba LABS

ELI-NP

Photo-Nuclear Reaction

is important as one of fundamental reactions for studying

- Nuclear structures/reactions
- Astro-nuclear physics, particle physics, detector response
- Applications
  - Radiation shield, decommissioning, reactions in nuclear reactors
  - Photo-activation analysis, nondestructive inspection
  - γ-imaging、CT-diagnostics、biological effects
  - Homeland security、inspection of fission or explosive material
  - Medical RI production by photo-irradiation
  - Nuclear reaction/gamma radiation in thunder volts

Data and theoretical predications are used in simulations of various fields.

99.99999% of the elements in the universe consists of nuclei below A=60

^{12}C and ^{16}O are still important to measure

Oxygen (^{16}O) forms 65% (30%) of the human body (Earth)

and Carbon (^{12}C) 8% (0.02%)

α-decay of IVGDR in ^{12}C or ^{16}O are not known well.

^{16}O	65%	30%
^{12}C	8%	0.02%

※^{16}O (^{12}O) isotopic abundance: 99.8 (98.9)%

\12C and 16O are still important to measure

Oxygen (^{16}O) forms 65% (30%) of the human body (Earth)

and Carbon (^{12}C) 8% (0.02%)

α-decay of IVGDR in ^{12}C or ^{16}O are not known well.

α-decay to low-lying ($T = 0$) states is isospin-forbidden.

$$^{16}\mathrm{O}(T=0) + \gamma \rightarrow {}^{16}\mathrm{O}^*(\mathrm{IVGDR}: T=1) \not\rightarrow {}^{12}\mathrm{C}(T=0) + \alpha(T=0)$$

isospin forbidden decay

requires implementation of isospin-symmetry breaking by Coulomb interaction

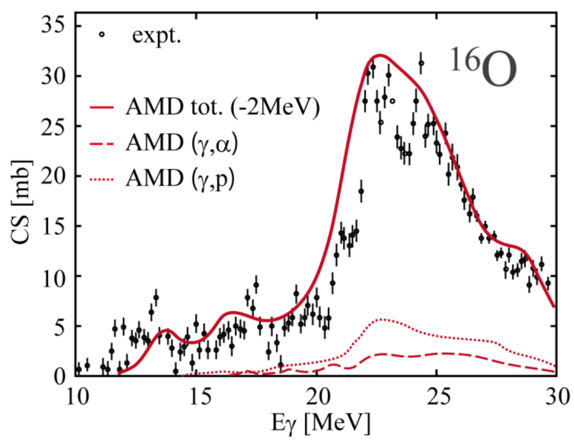

prediction by AMD
M. Kimura et al.,

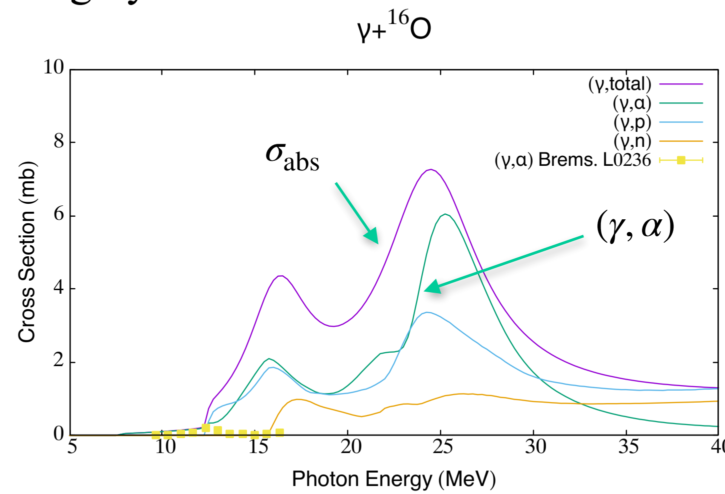

calculation with TALYS
(default parameters)

Decay of IVGDR

time dependent description of the decay of a collective excitation

an ordered motion to a random motion

γ

IVGDR

collective motion

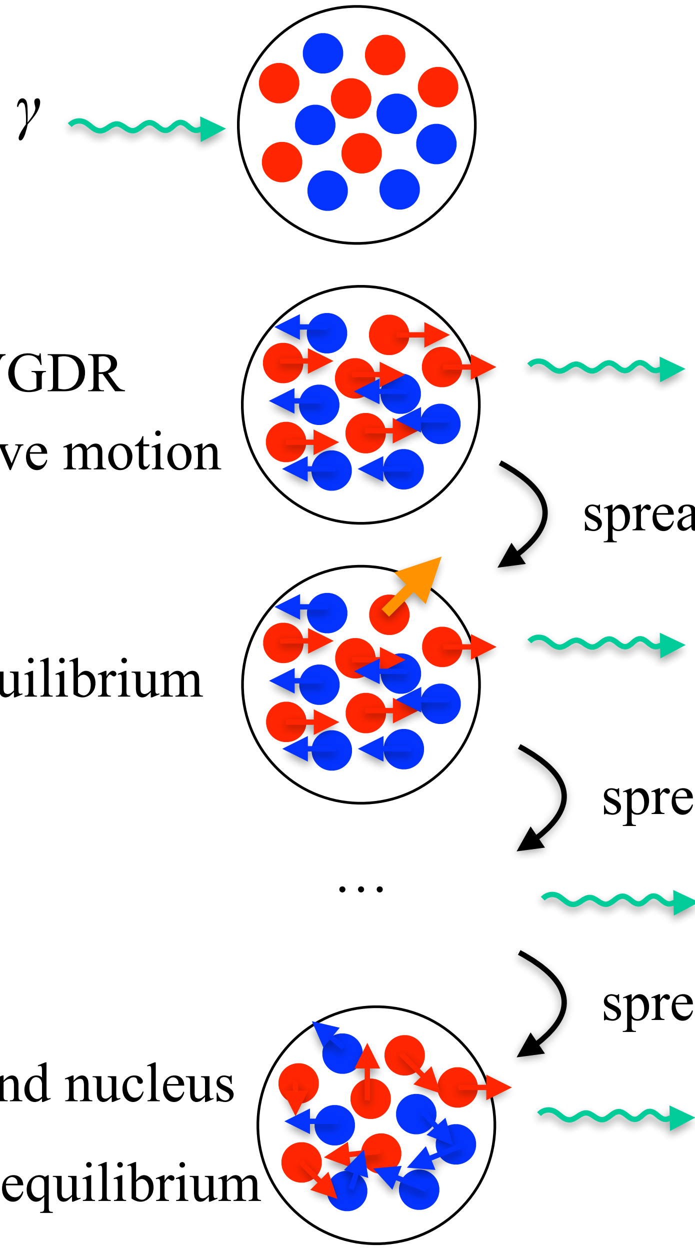

direct decay

(n,p,α,γ,..)

spreading

pre-equilibrium

pre-equilibrium decay

spreading

…

pre-equilibrium decay

spreading

compound nucleus

thermal equilibrium

compound (statistical) decay

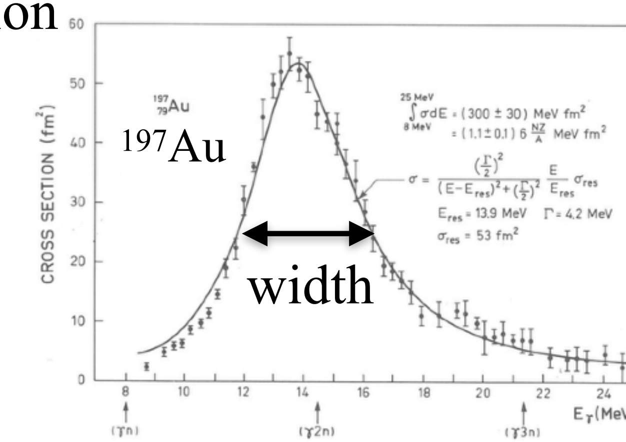

Intergalactic Propagation of Ultra-High-Energy Cosmic Rays

Cosmic Rays

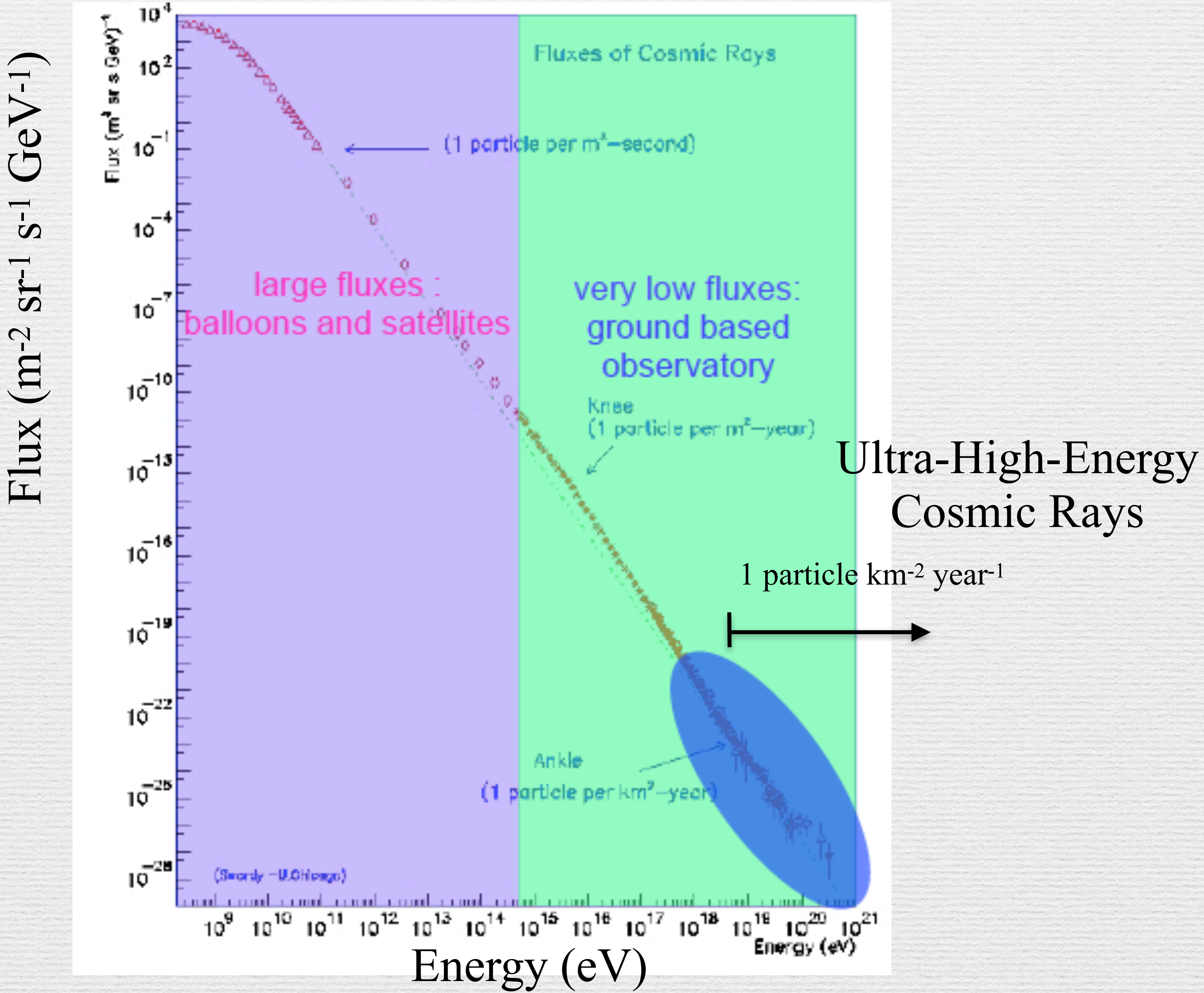
Fluxes of Cosmic Rays
(1 particle per m²—second)
large fluxes :
balloons and satellites
very low fluxes:
ground based
observatory
Knee
(1 particle per m²—year)
Ankle
(1 particle per km²—year)
Flux (m² sr s GeV)⁻¹
Energy (eV)
Flux (m-2 sr-1 s-1 GeV-1)
Energy (eV)
Ultra-High-Energy
Cosmic Rays
1 particle km-2 year-1

Ultra-High-Energy Cosmic Rays (UHECRs) [PDG2018]

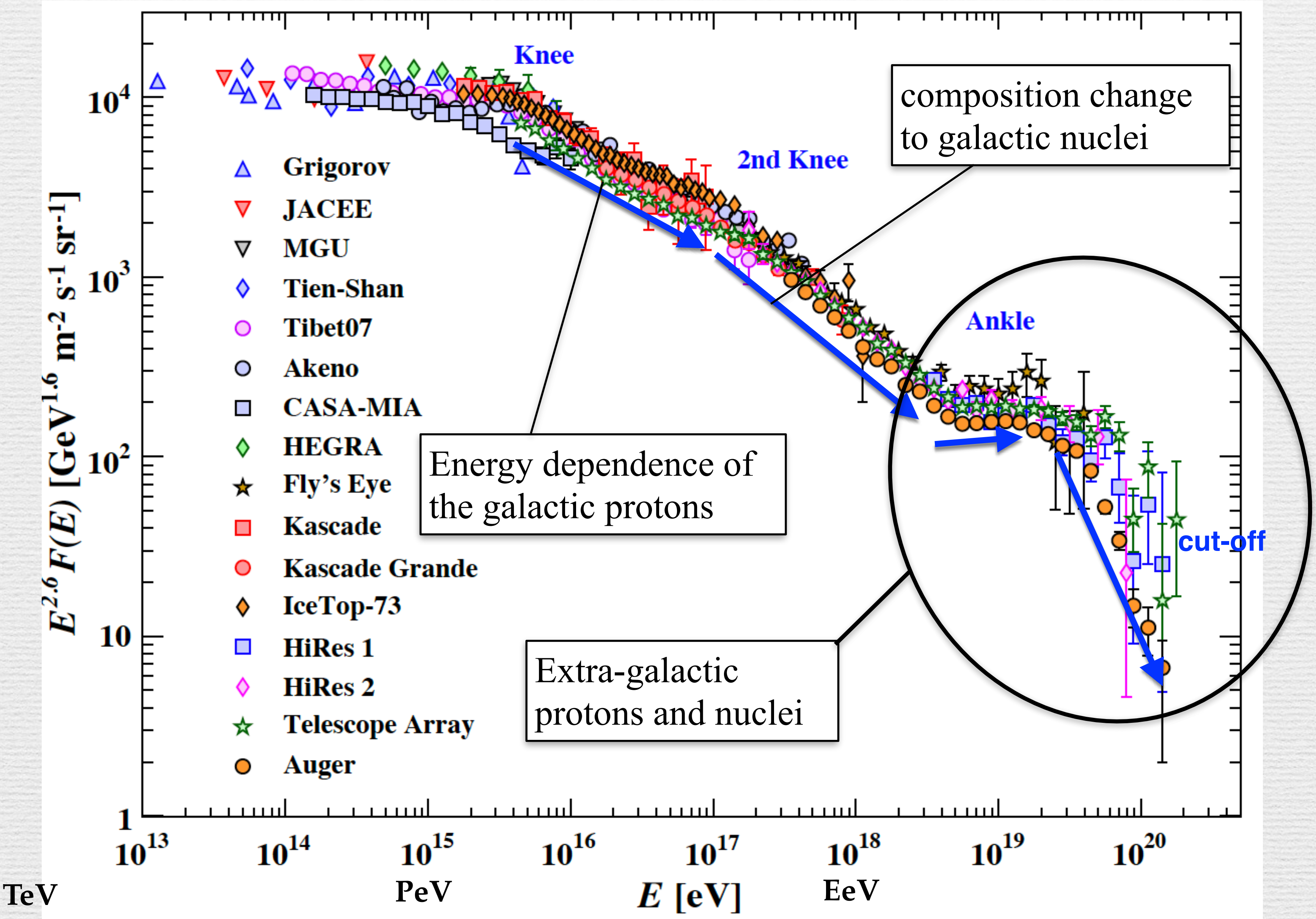

Observation of UHECRs

Extended Air Shower (EAS)

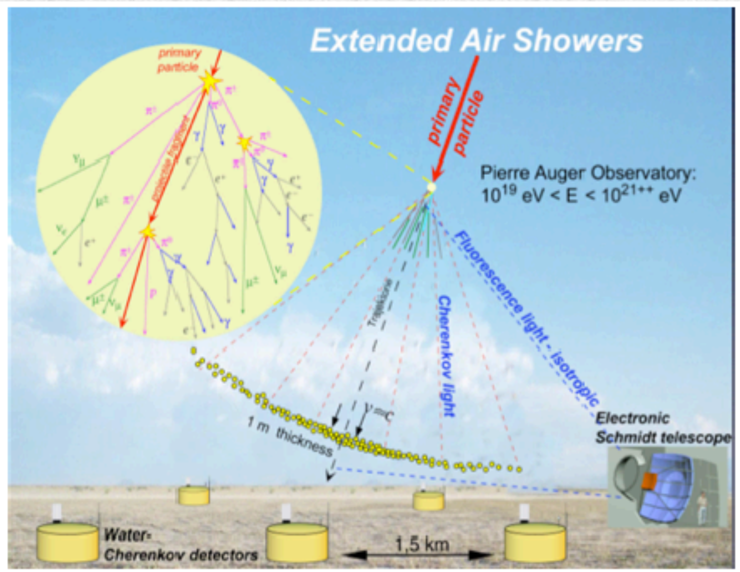

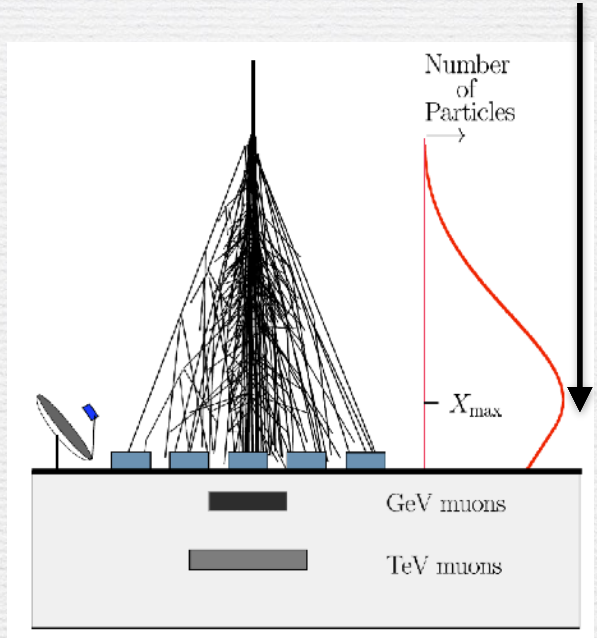

X_{max}:
atmospheric depth at the maximum number of particles of the air shower

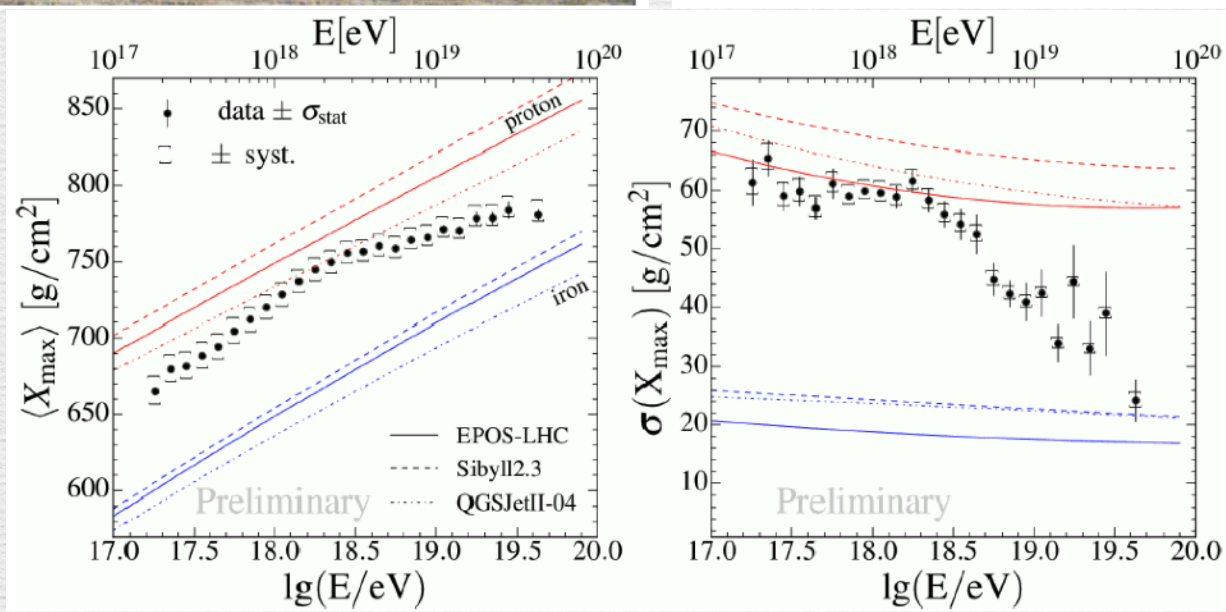

[mol18]
[gor18]

The observed mass tends to become heavier as the energy increase at the highest energy.

Intergalactic Propagation of UHECR Nuclei

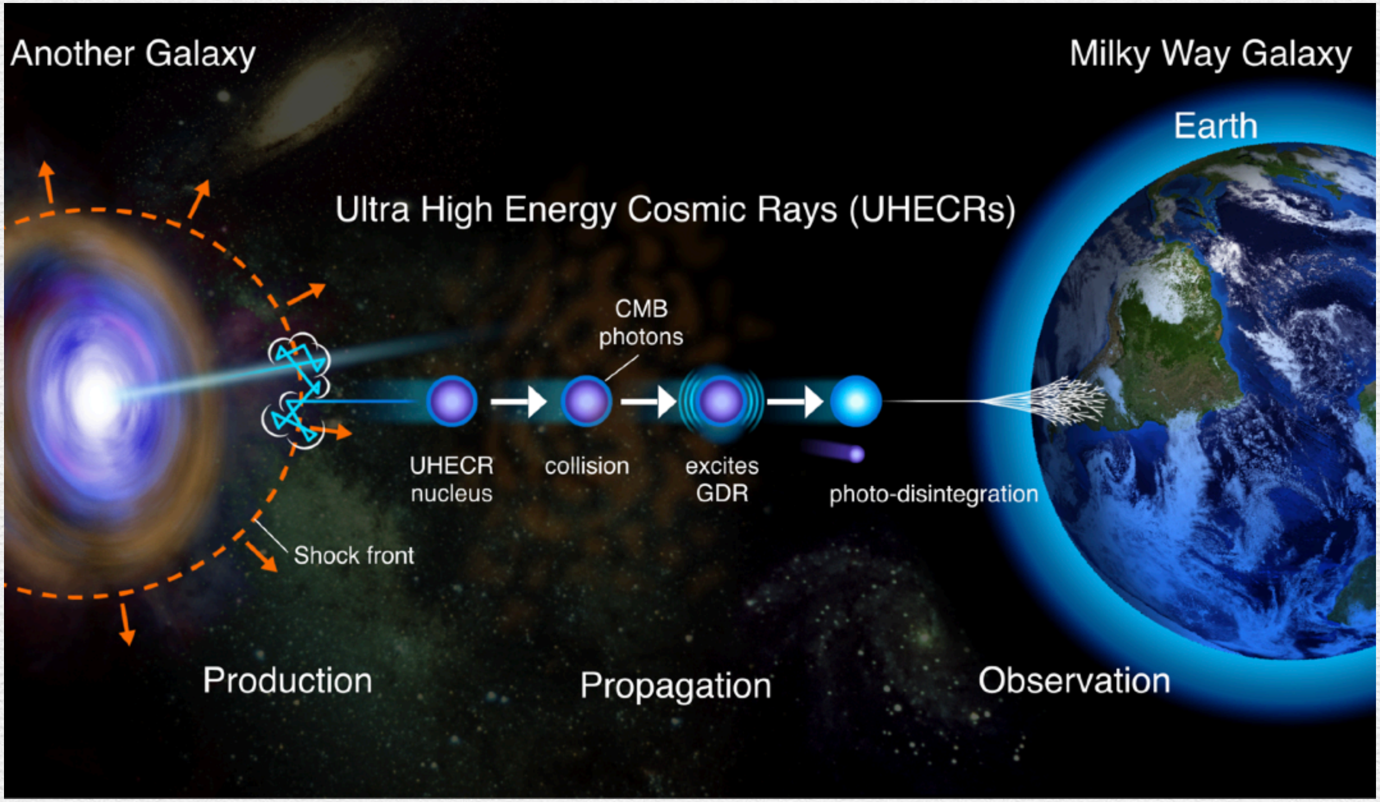

Photo-nuclear reactions govern the maximum travel distance of UHECR nuclei and their composition/ energy evolution in the inter-galactic propagation.

Cosmic Microwave Background (CMB)

WMAP
T=2.73 K

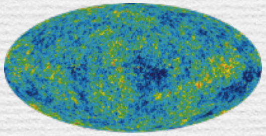

GZK cut-off

Photo-disintegration Pass of ^{56}Fe

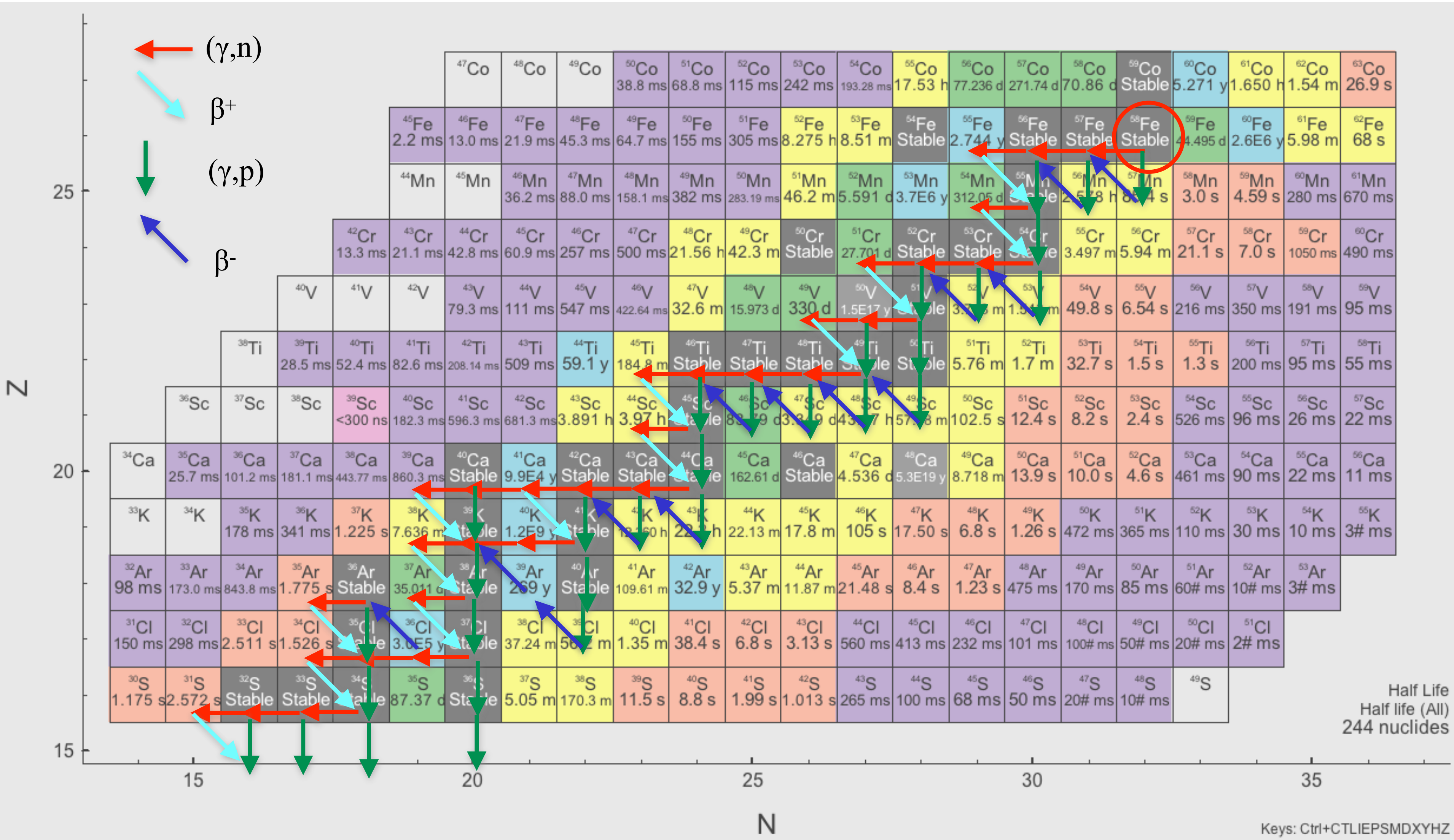

(γ,xn), (γ,α) reactions also take place.

Unstable nuclei ($T_{1/2}$ > 1 min) also contribute.

UHECR: Intergalactic Propagation

1 Mpc = 3.26×10^6 light year

the Milky Way Galaxy

0.03 Mpc

0.03 Mpc for $T_{1/2} = 5$ min at $\gamma = 10^{10}$

UHECR: Intergalactic Propagation

the Milky Way Galaxy

Andromeda Galaxy

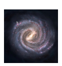

0.78 Mpc

UHECR: Intergalactic Propagation

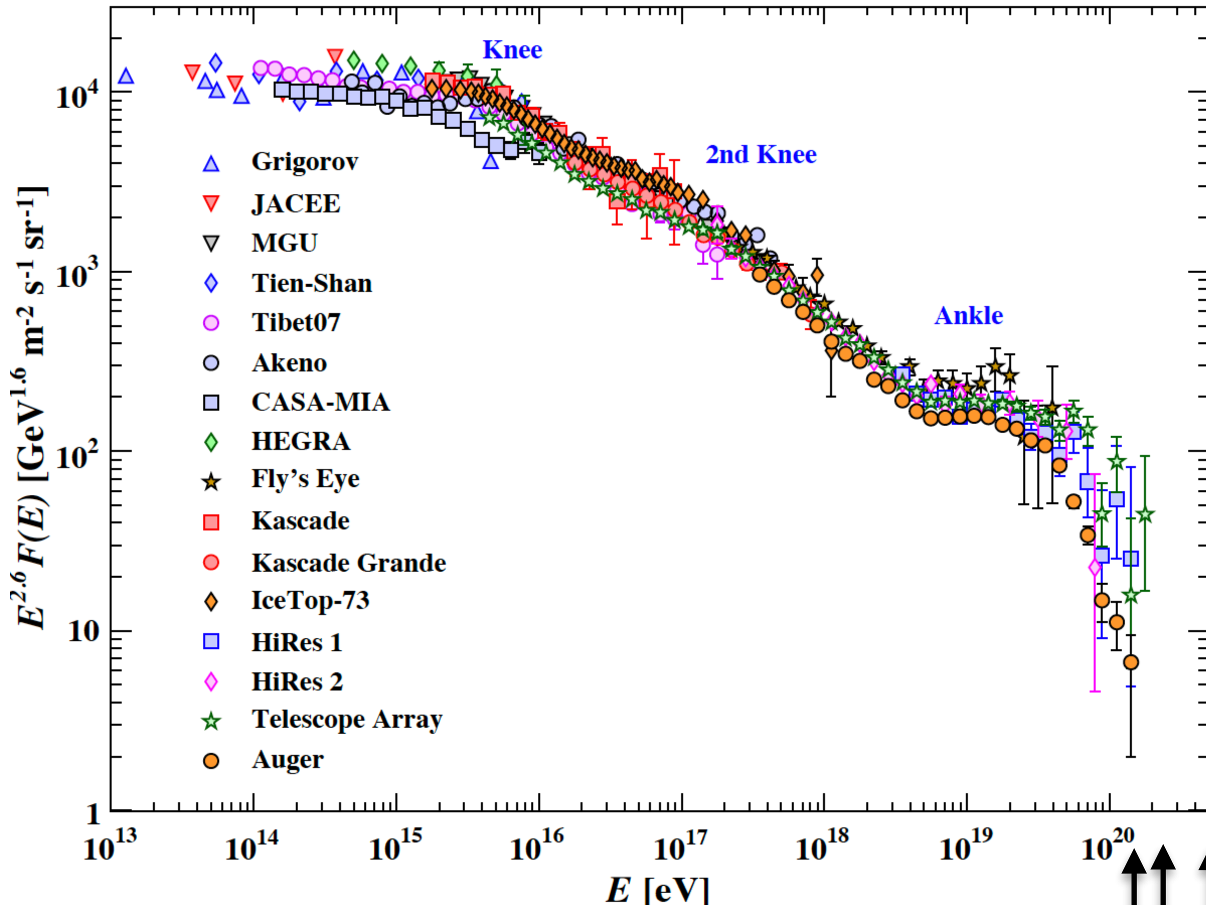

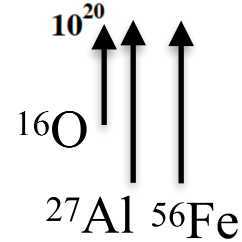

$$\gamma = \frac{E}{M} = 10^{10}$$

	mass
^{16}O	14.9 GeV/c^2
^{27}Al	25.1 GeV/c^2
^{56}Fe	52.1 GeV/c^2

UHECR: Intergalactic Propagation

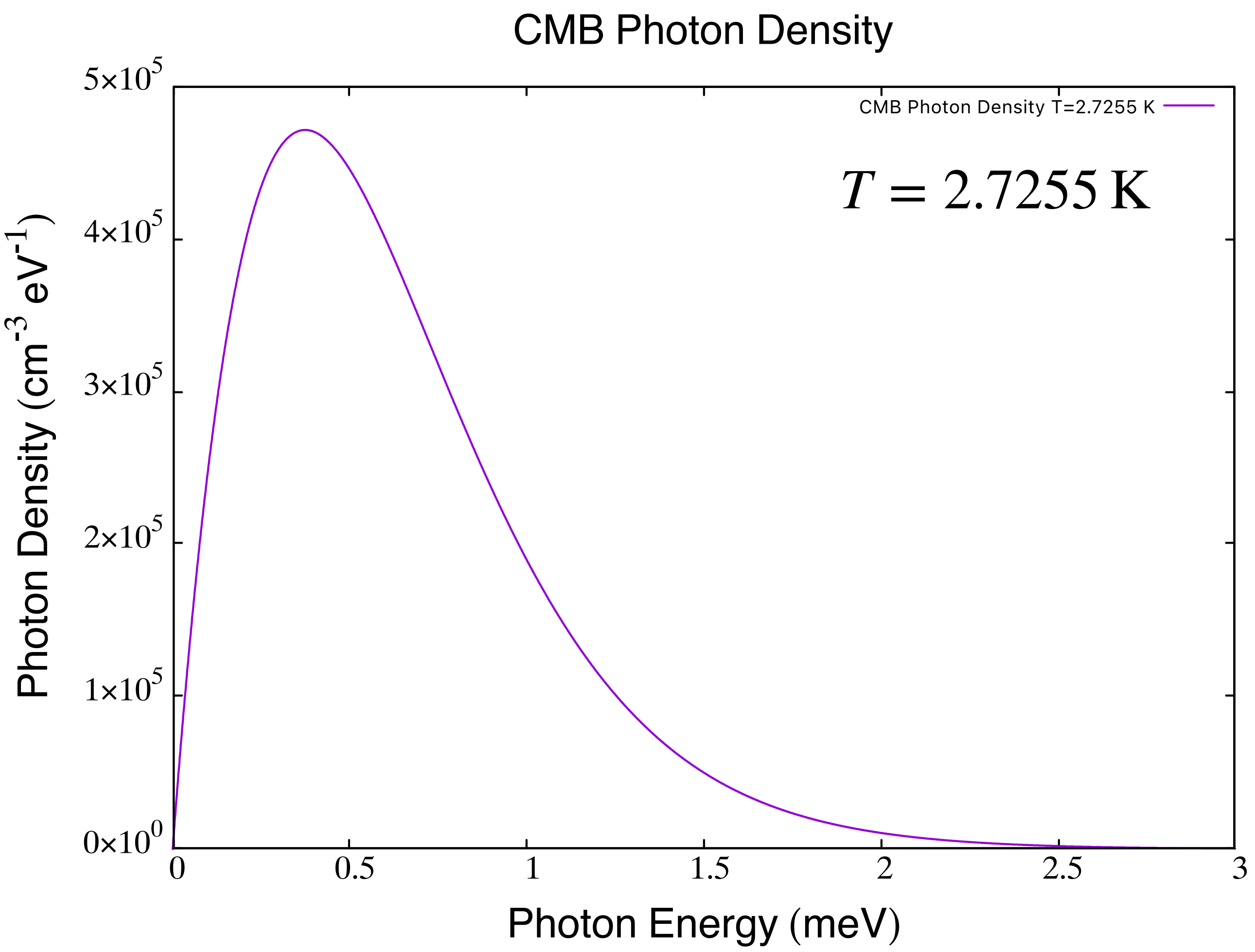

UHECR: Intergalactic Propagation

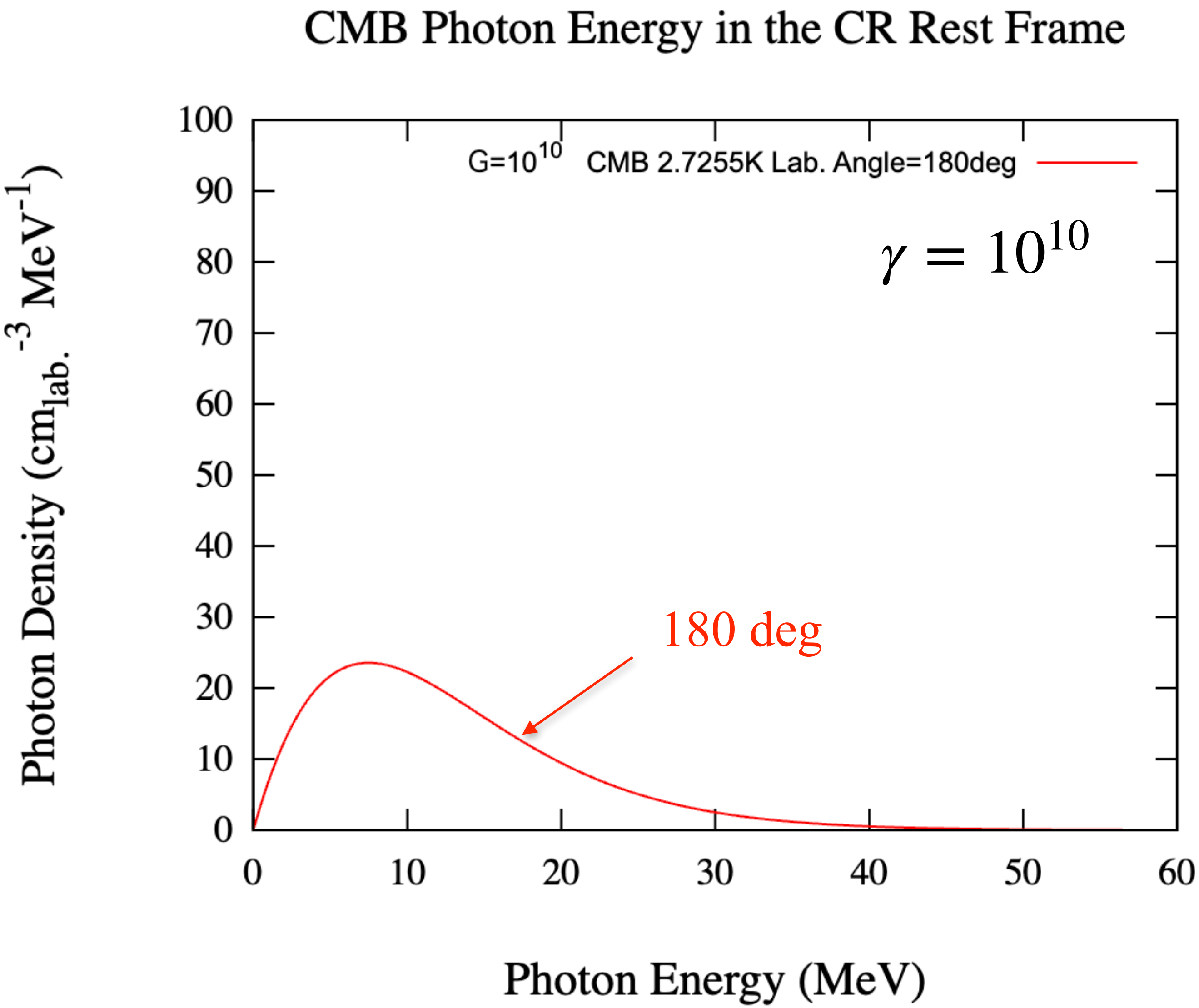

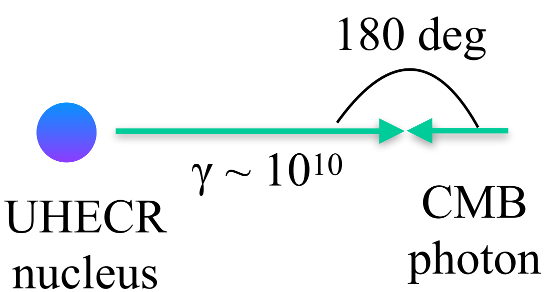

UHECR: Intergalactic Propagation

CMB Photon Energy in the CR Rest Frame

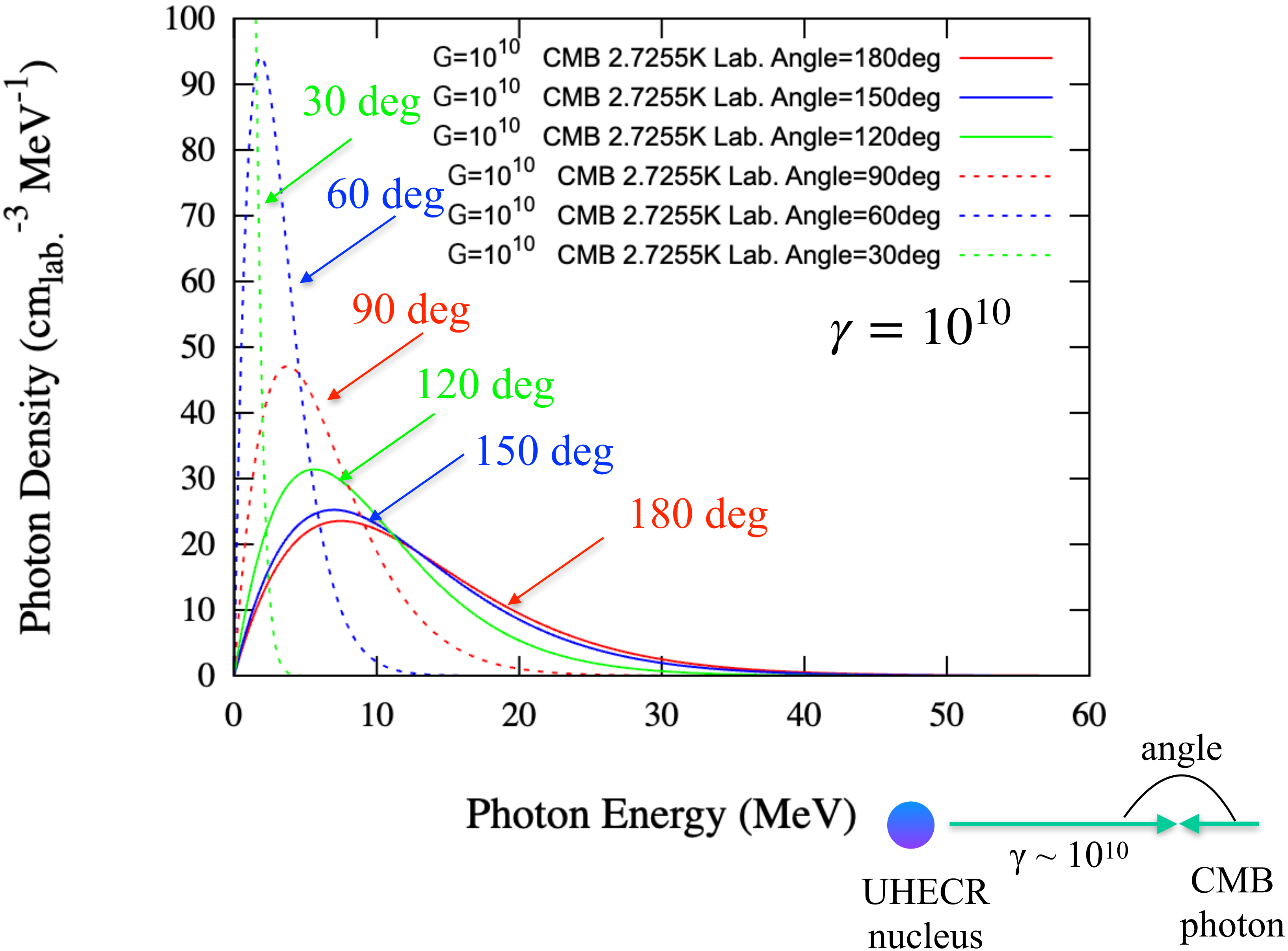

UHECR: Intergalactic Propagation

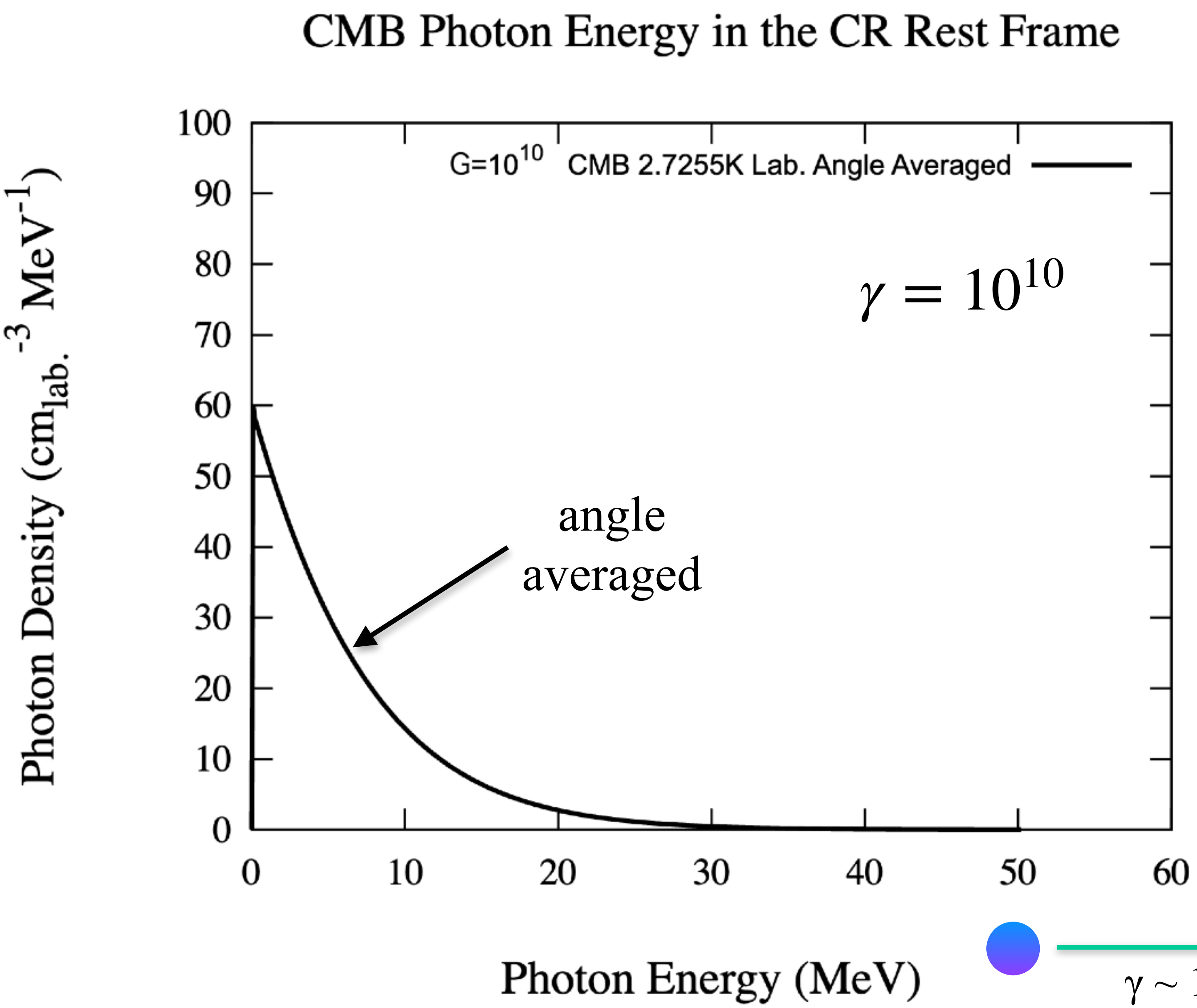

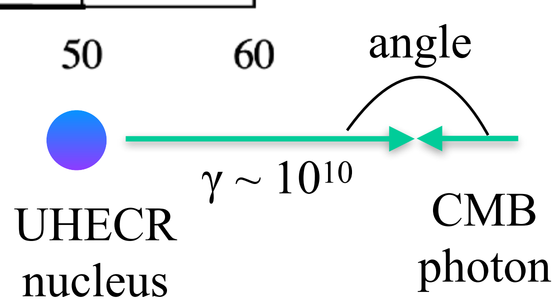

UHECR: Intergalactic Propagation

$^{16}O \quad \gamma = 10^{10}$

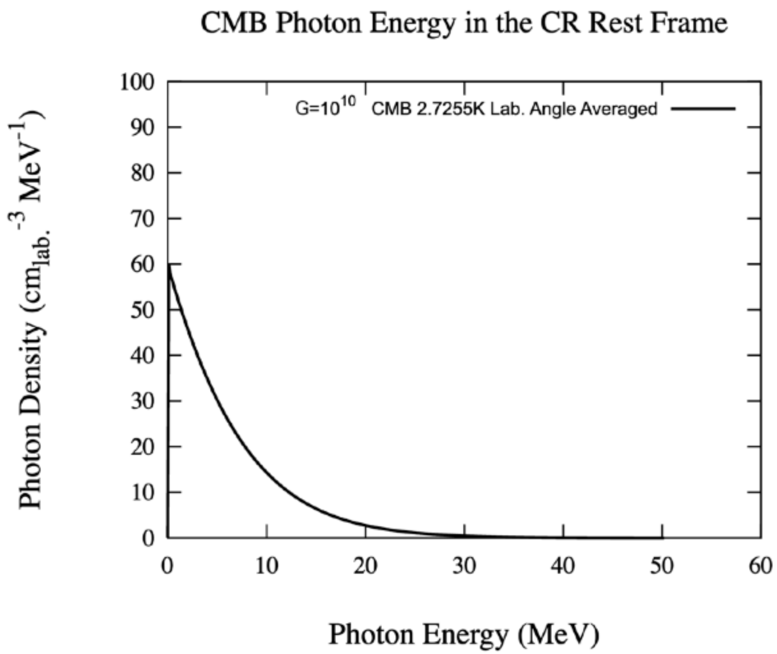

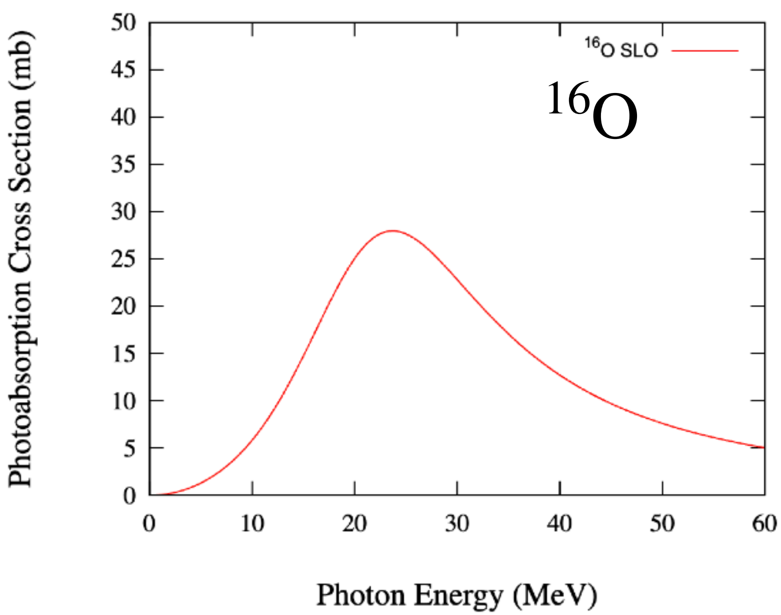

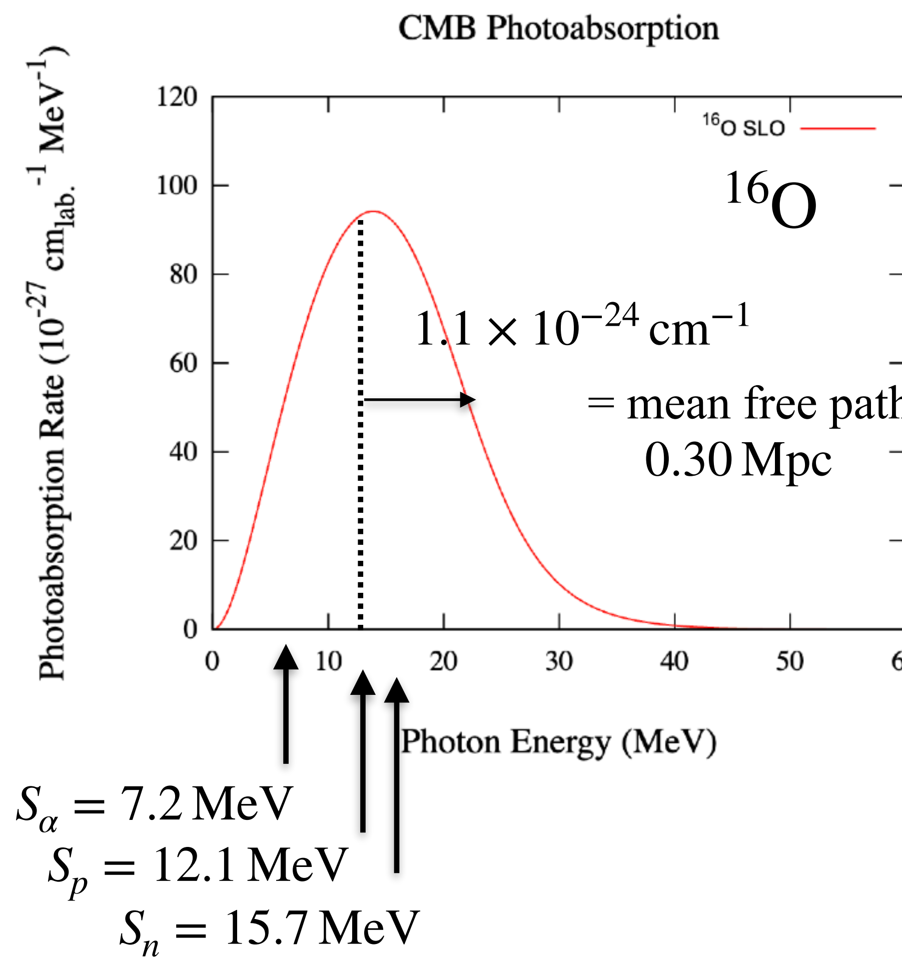

UHECR: Intergalactic Propagation

^{27}Al $\gamma = 10^{10}$

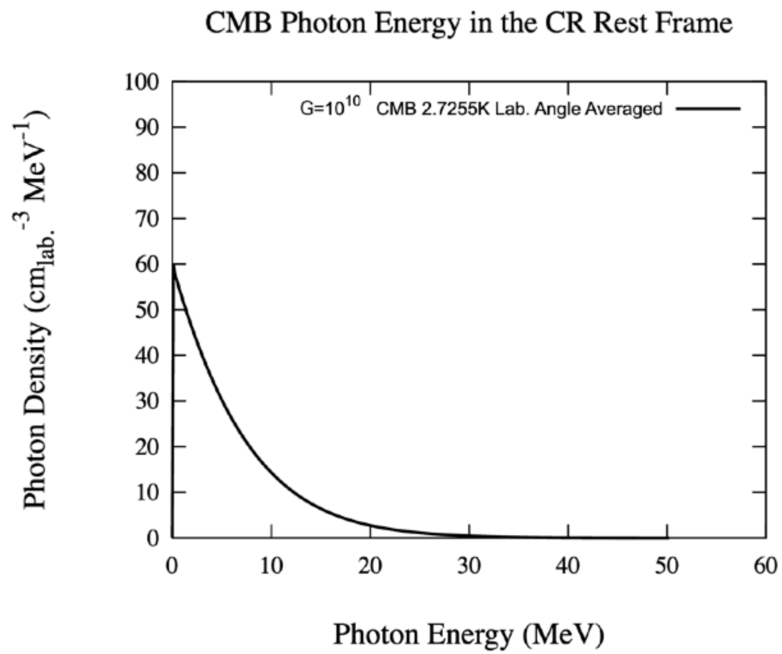

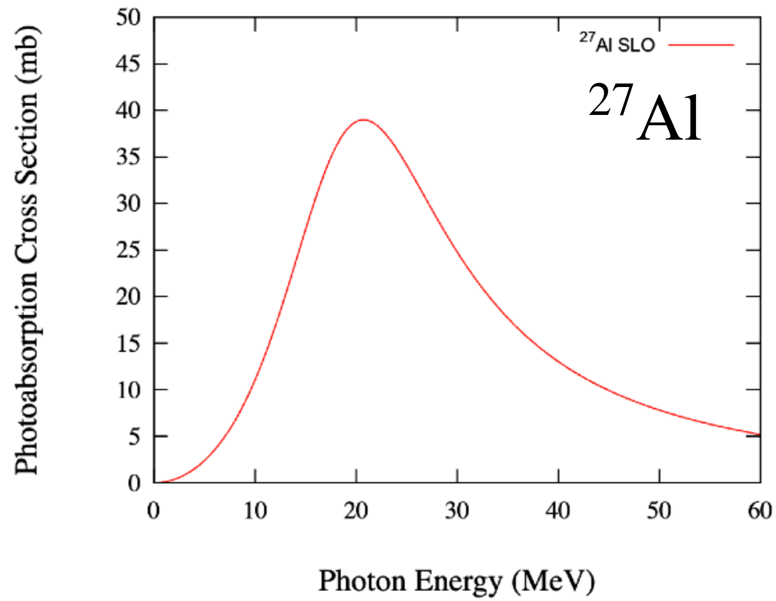

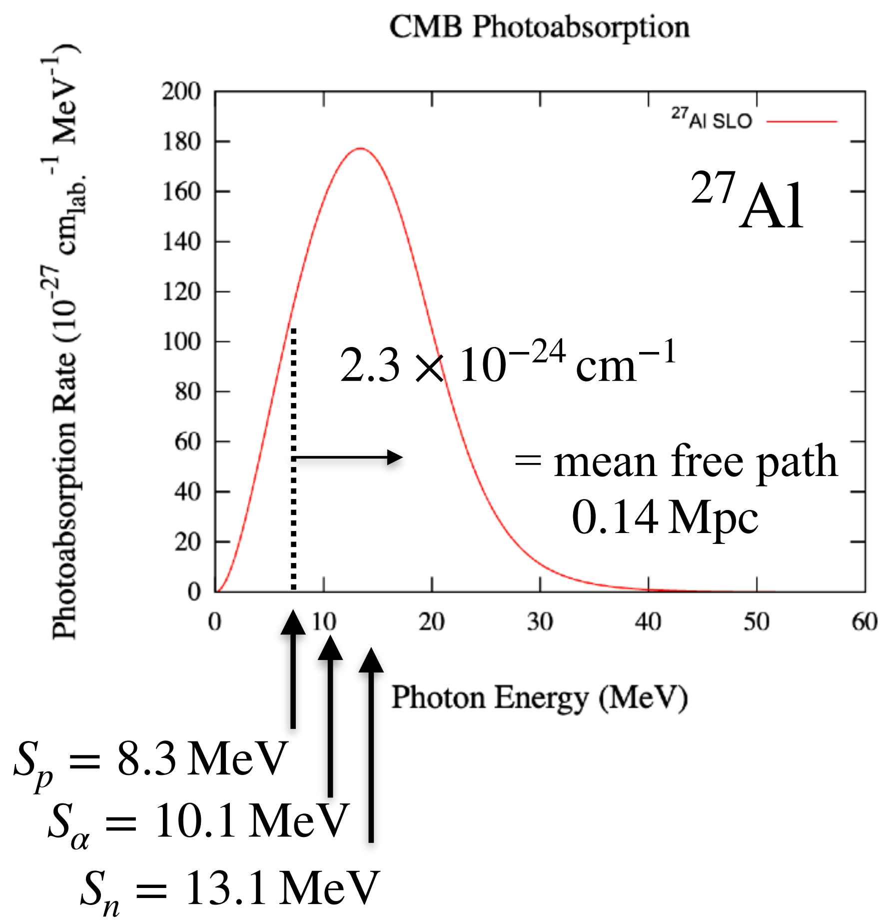

UHECR: Intergalactic Propagation

$^{54}\mathrm{Fe}$ $\gamma = 10^{10}$

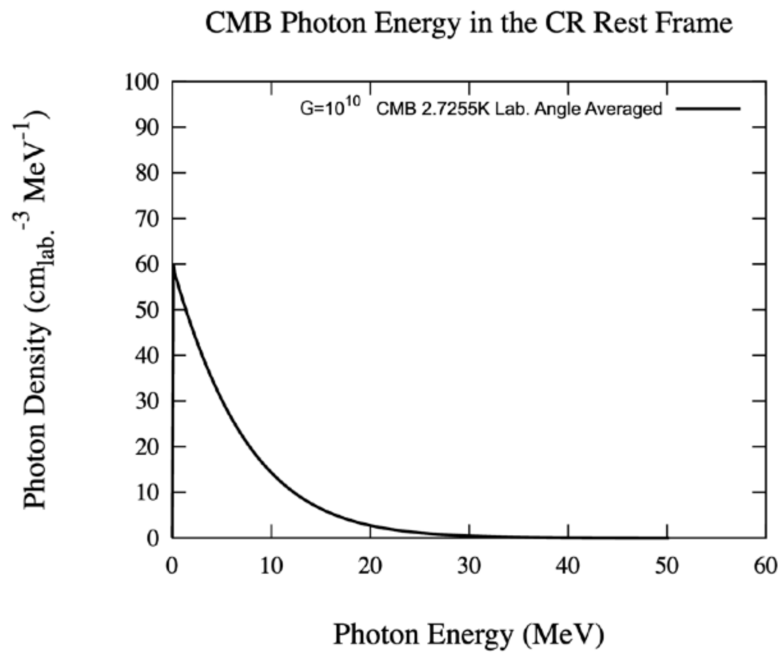

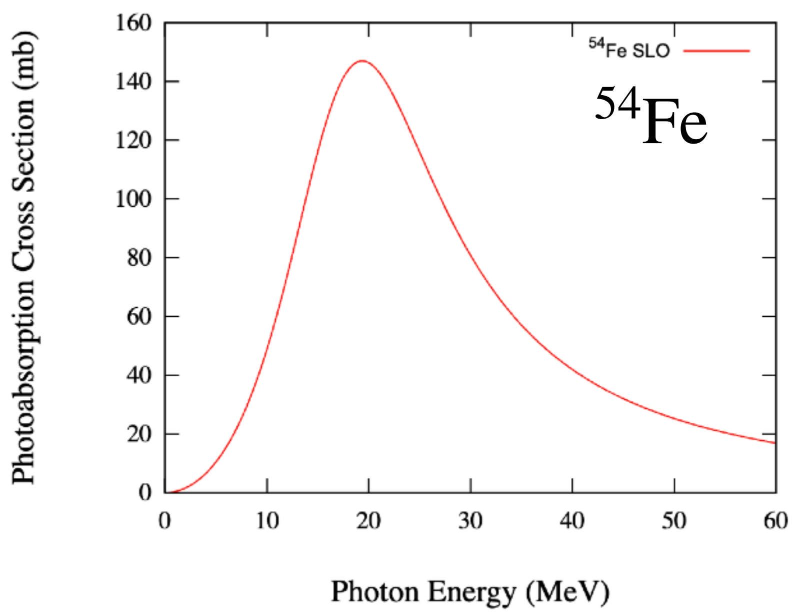

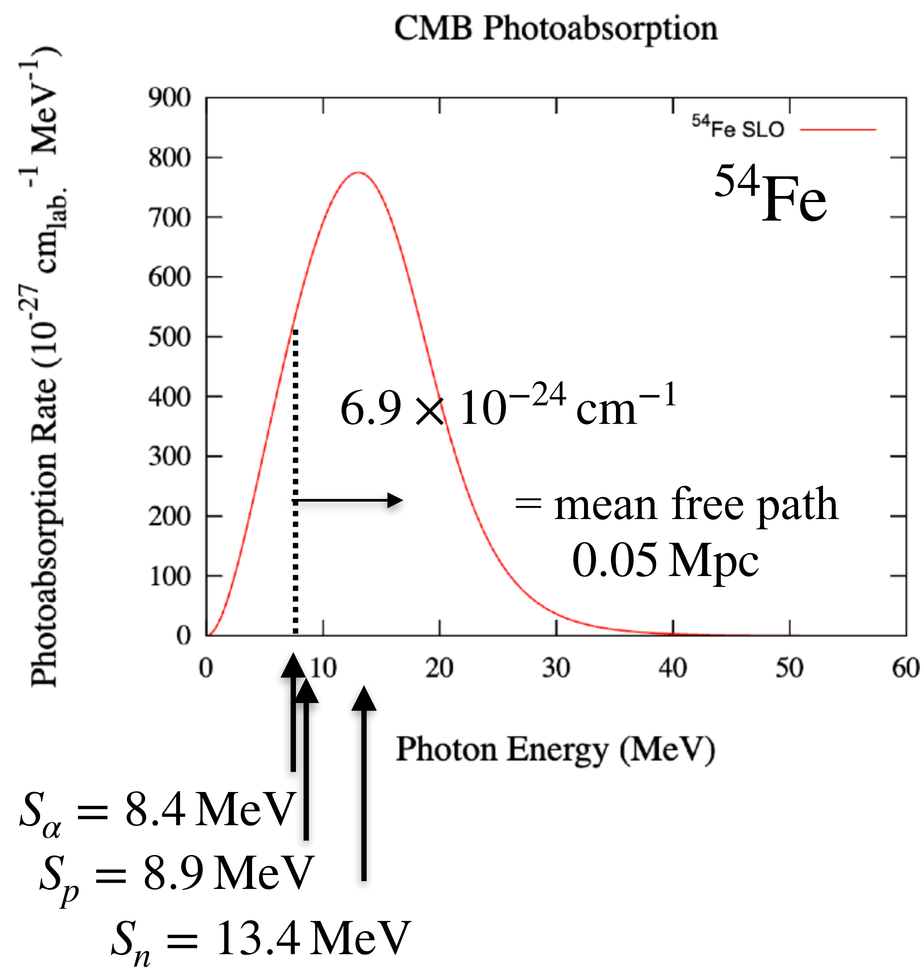

UHECR: Photo-Disintegration Mean Free Path

	$\gamma = 10^{9.5}$	$\gamma = 10^{10}$	$\gamma = 10^{10.5}$
^{16}O	53 Mpc	0.30 Mpc	0.083 Mpc
^{27}Al	5.9 Mpc	0.14 Mpc	0.055 Mpc
^{54}Fe	1.4 Mpc	0.034 Mpc	0.015 Mpc

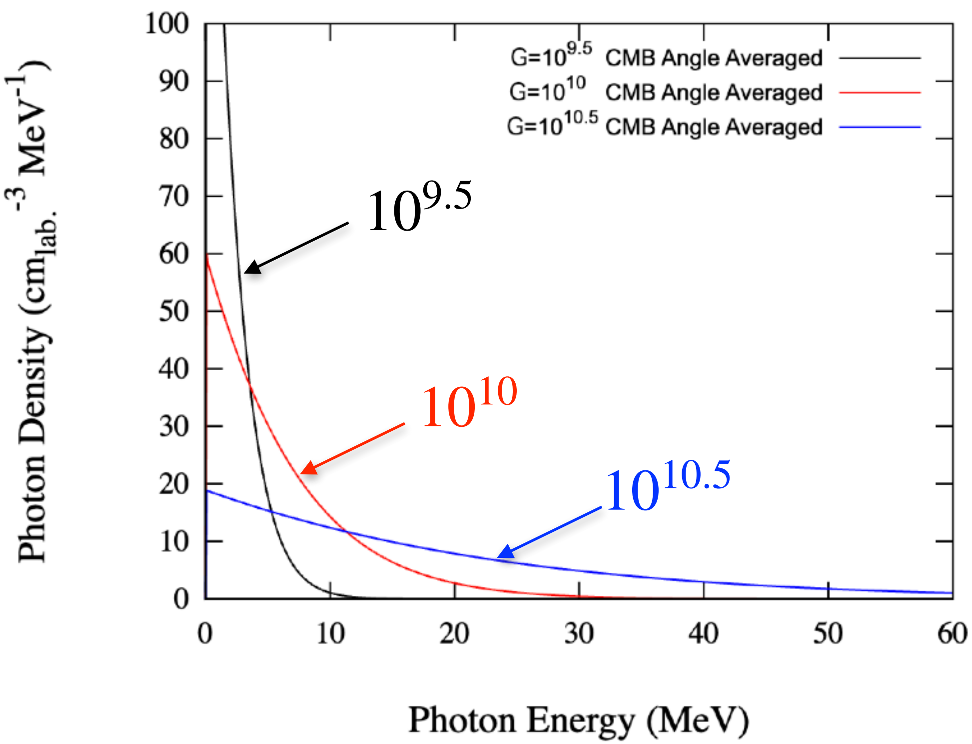

UHECR: Intergalactic Propagation by a Toy-Model Simulation

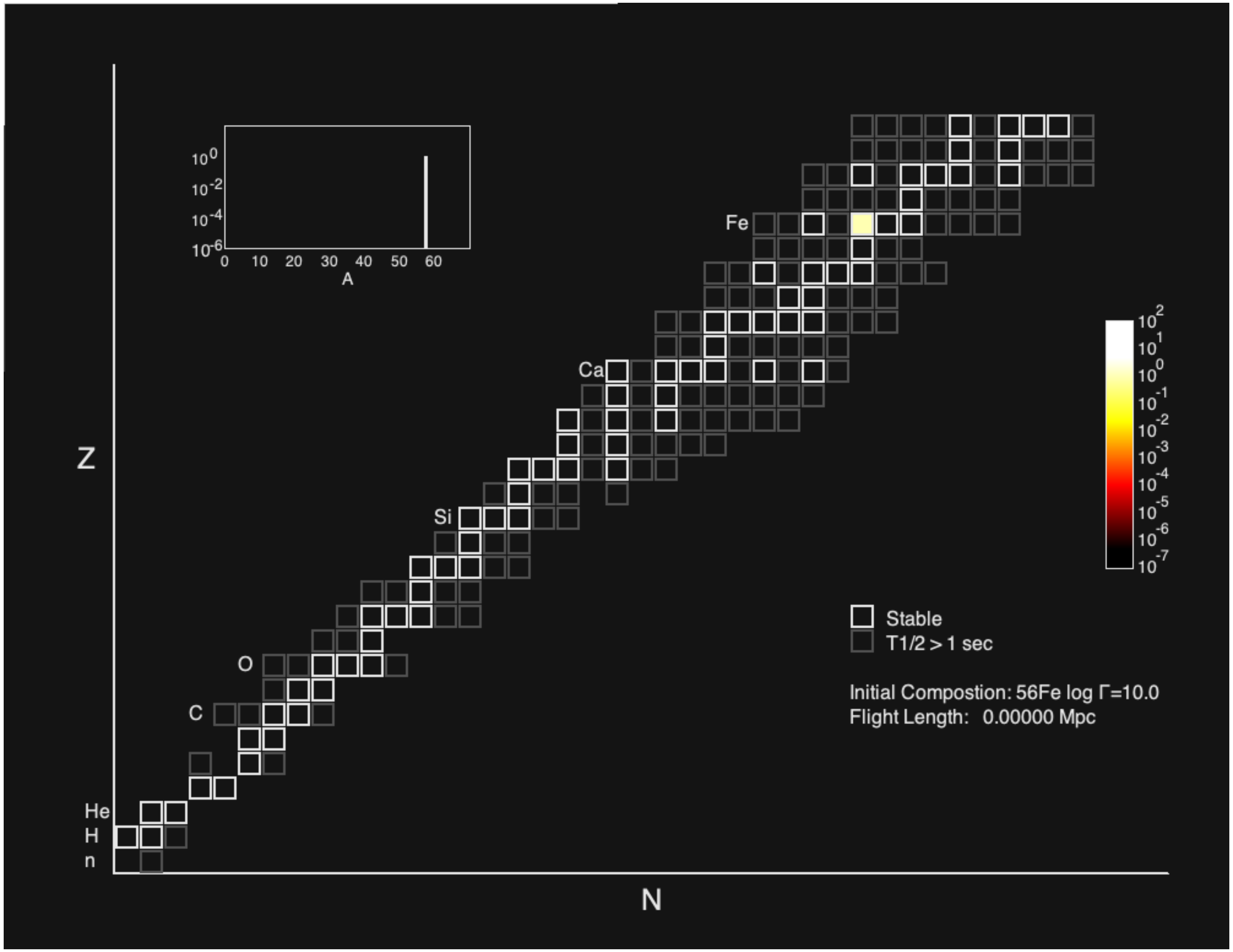

0 Mpc

initial condition

^{56}Fe

$\gamma = 10^{10}$

UHECR: Intergalactic Propagation by a Toy-Model Simulation

0.0001 Mpc

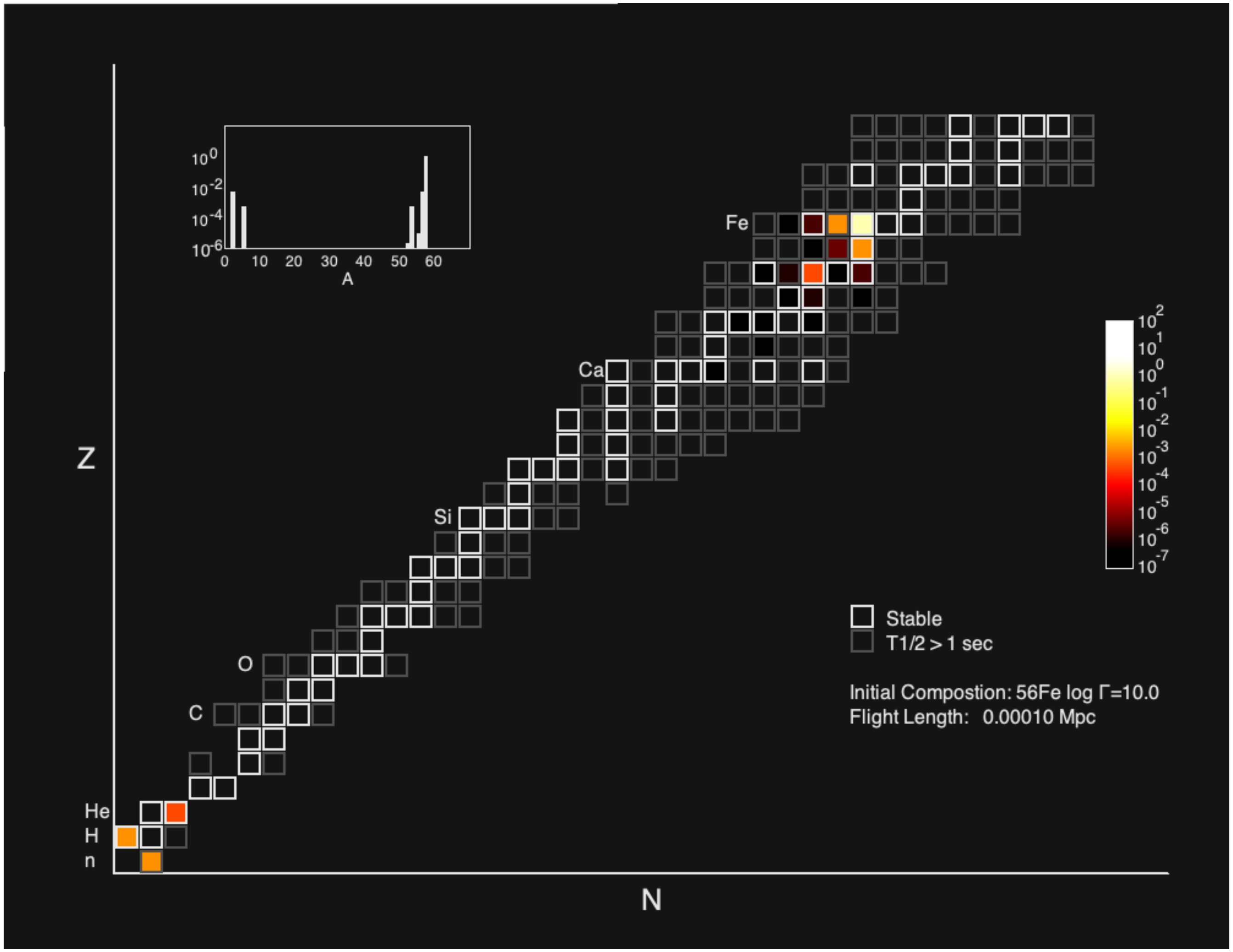

UHECR: Intergalactic Propagation by a Toy-Model Simulation

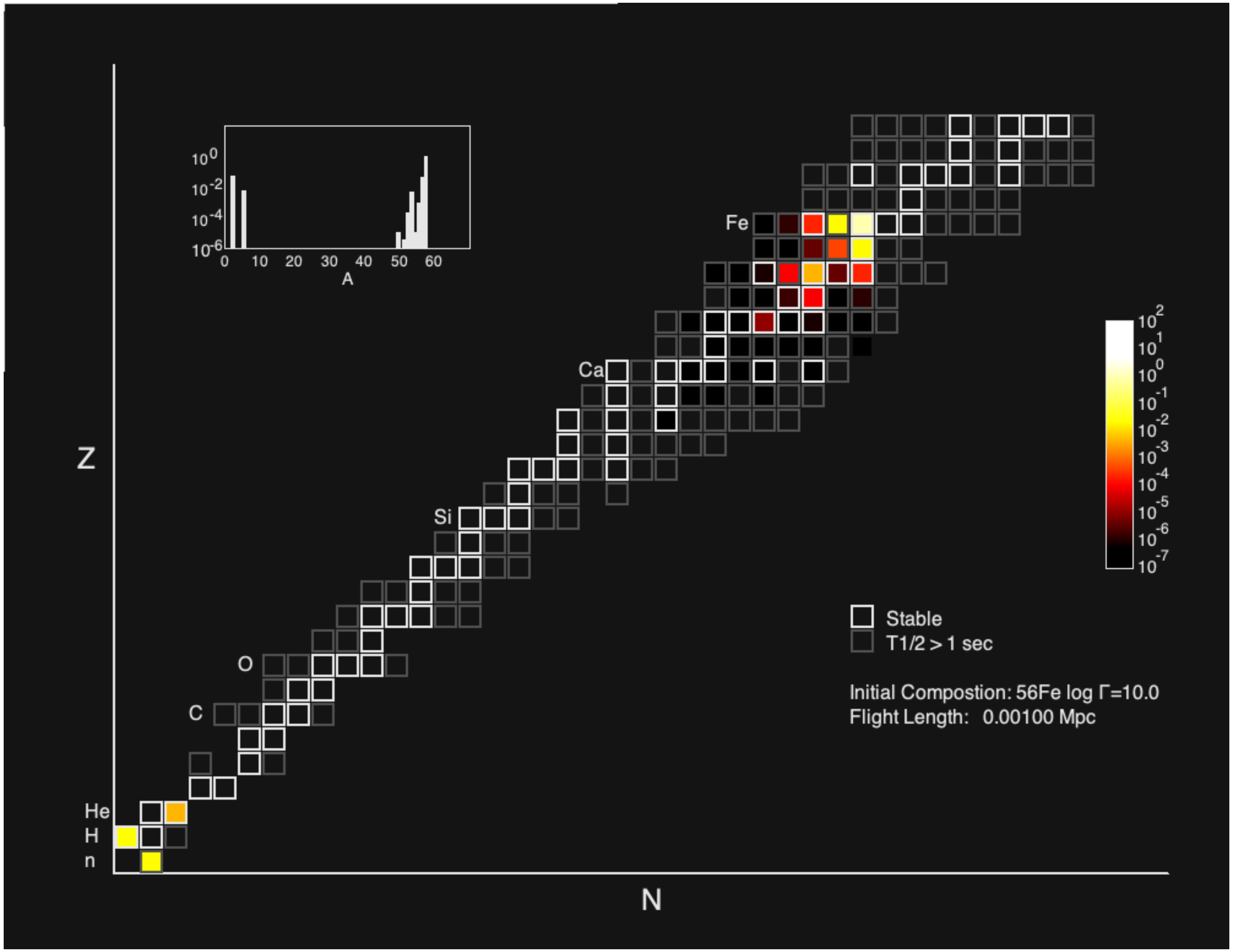

0.001 Mpc

UHECR: Intergalactic Propagation by a Toy-Model Simulation

0.01 Mpc

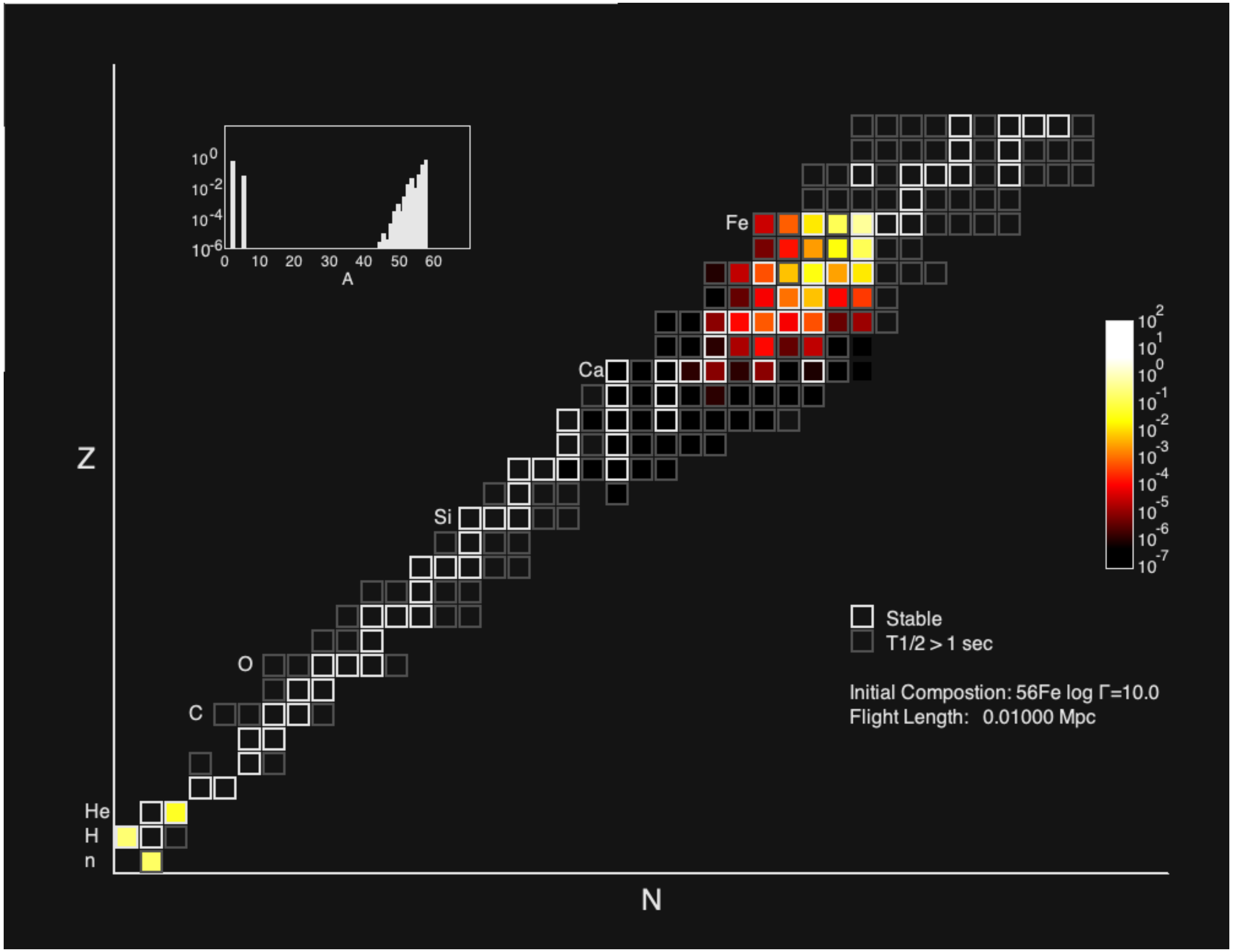

UHECR: Intergalactic Propagation by a Toy-Model Simulation

0.1 Mpc

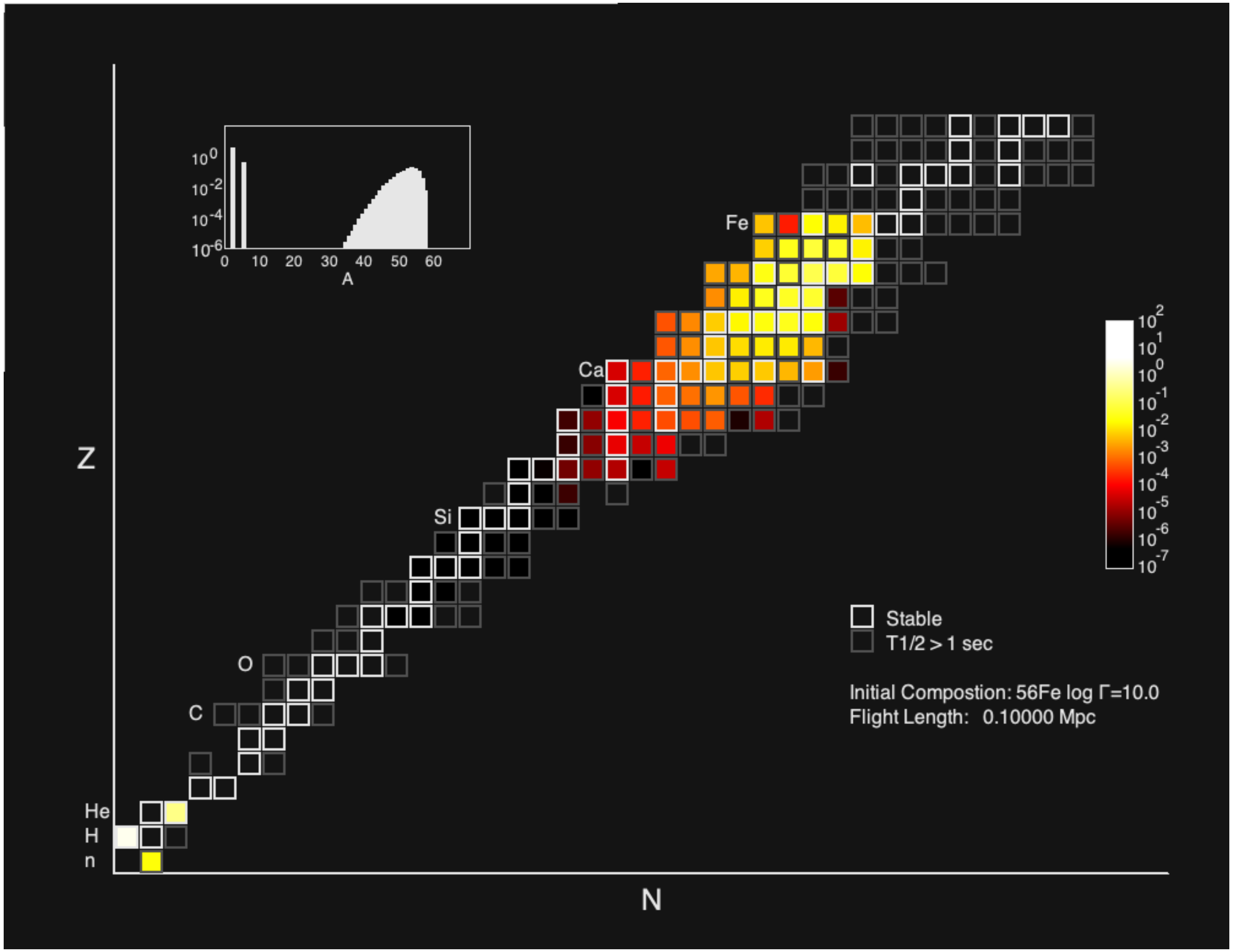

UHECR: Intergalactic Propagation by a Toy-Model Simulation

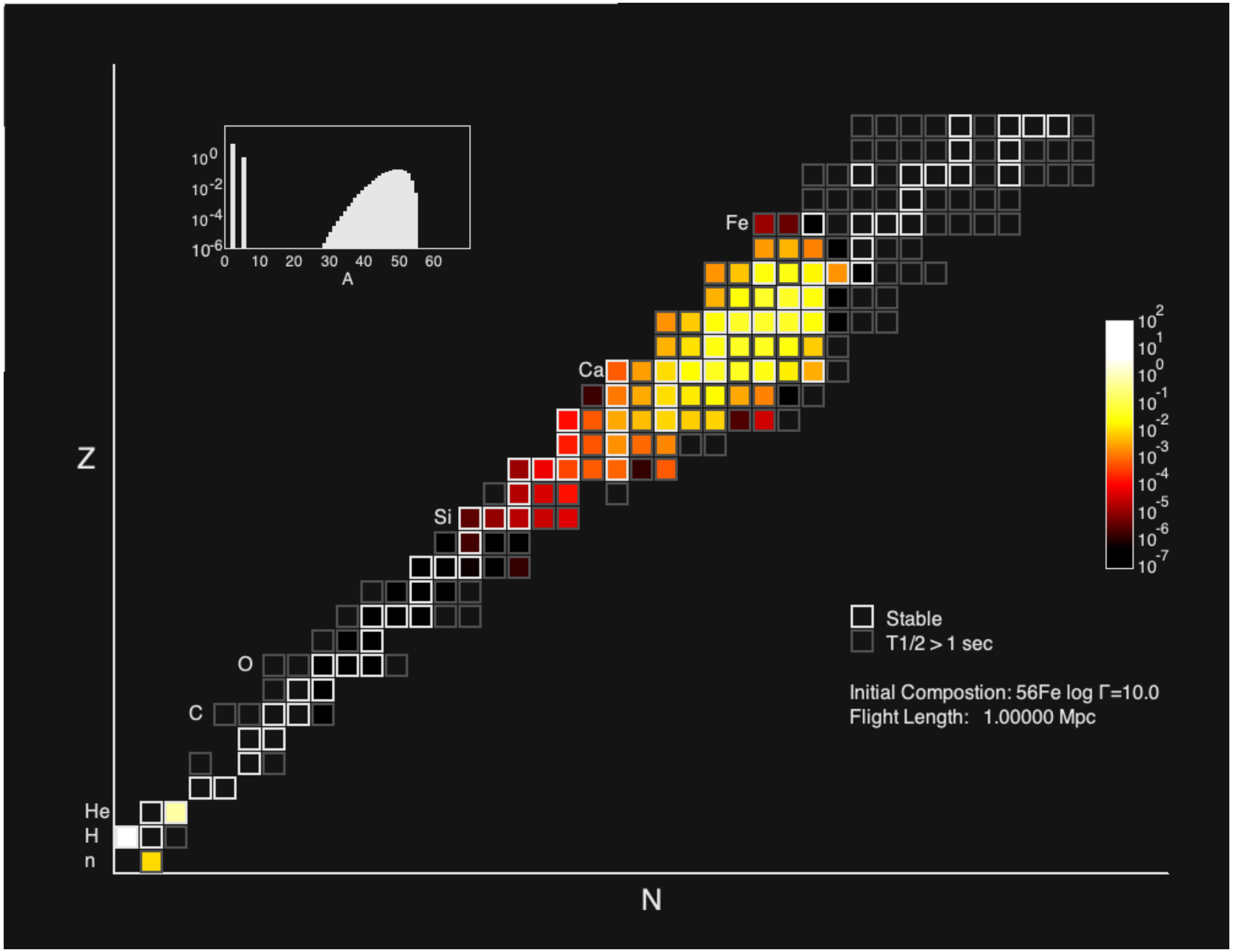

1 Mpc

UHECR: Intergalactic Propagation by a Toy-Model Simulation

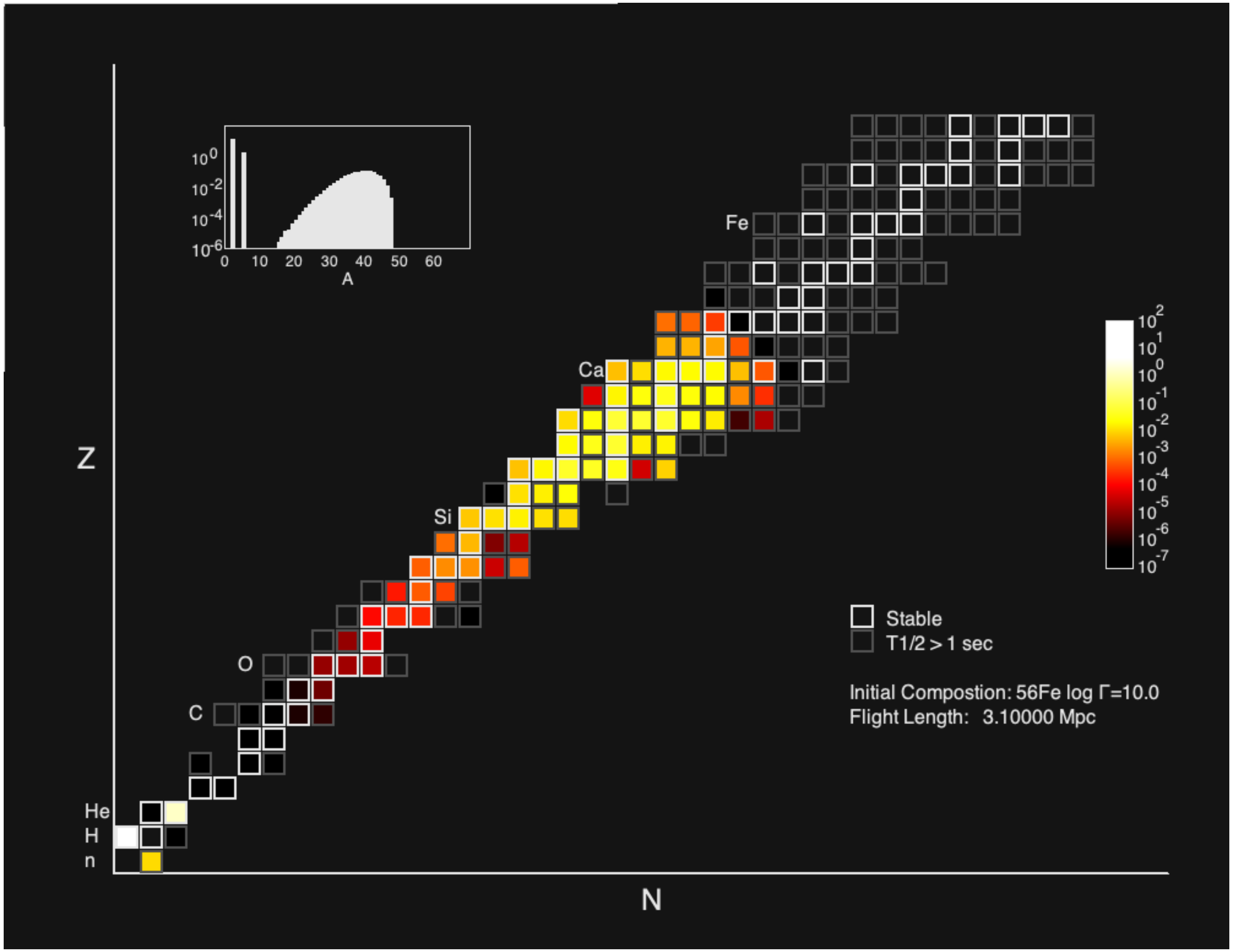

3 Mpc

UHECR: Intergalactic Propagation by a Toy-Model Simulation

10 Mpc

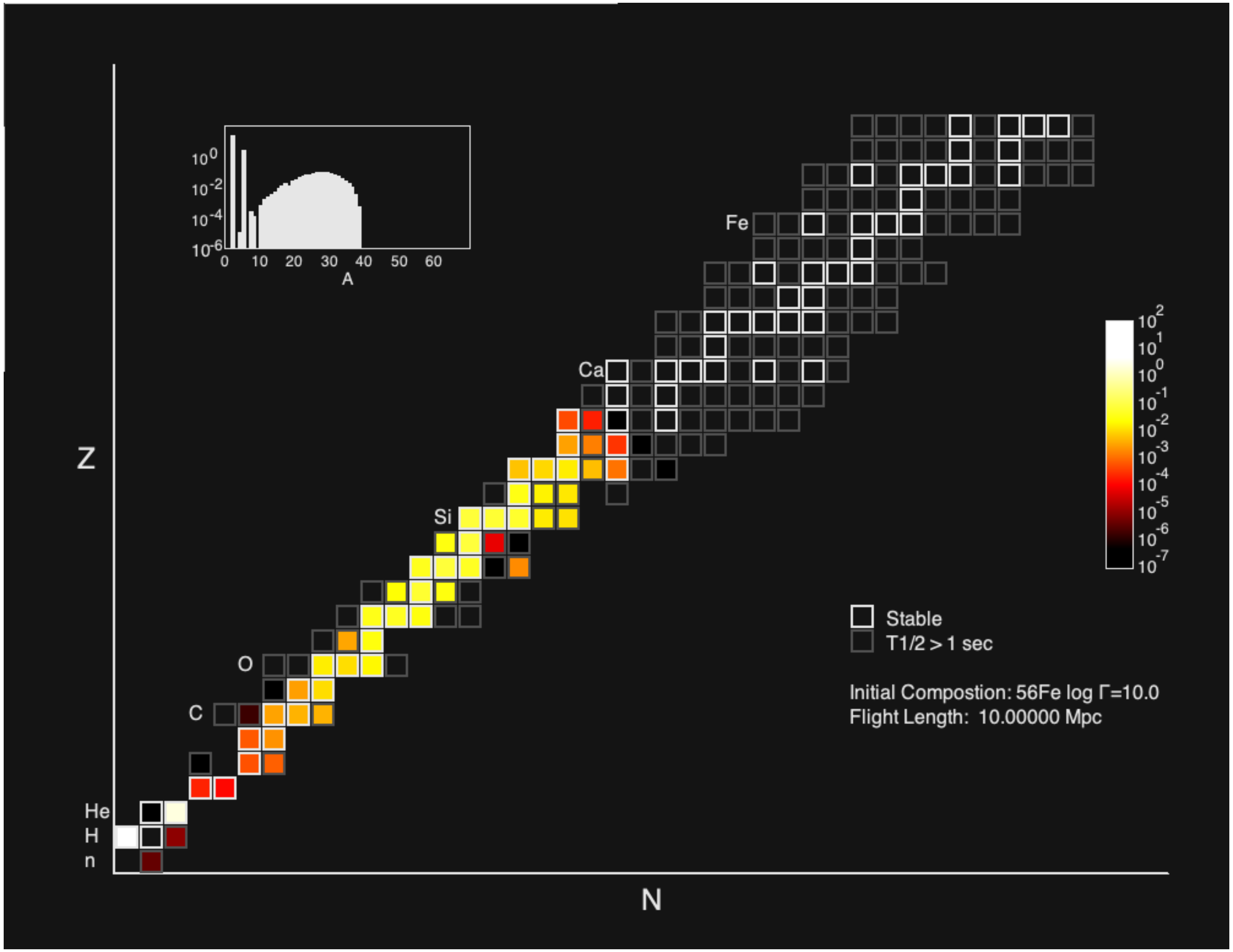

UHECR: Intergalactic Propagation by a Toy-Model Simulation

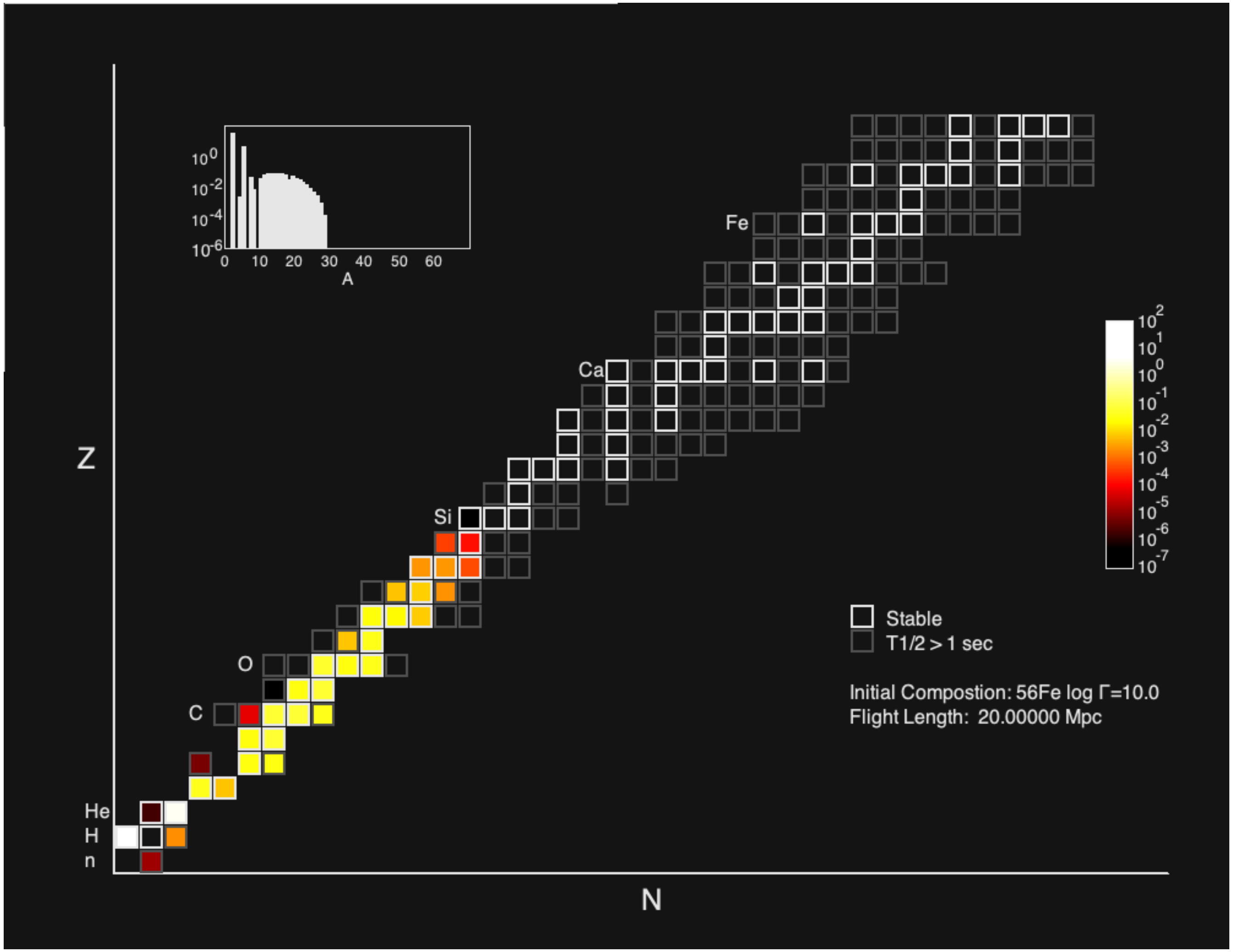

20 Mpc

UHECR: Intergalactic Propagation by a Toy-Model Simulation

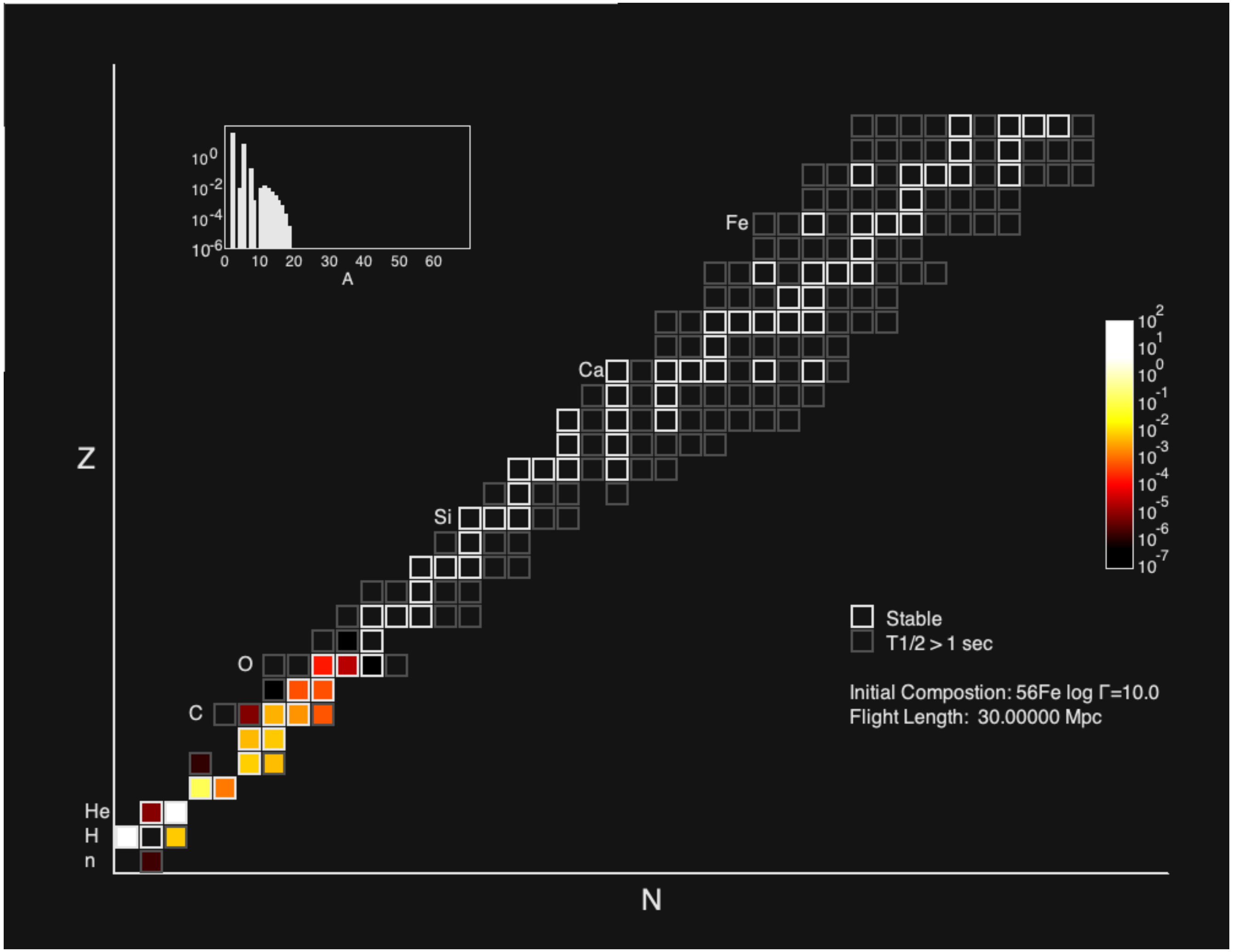

30 Mpc

UHECR: Intergalactic Propagation by a Toy-Model Simulation

300 Mpc

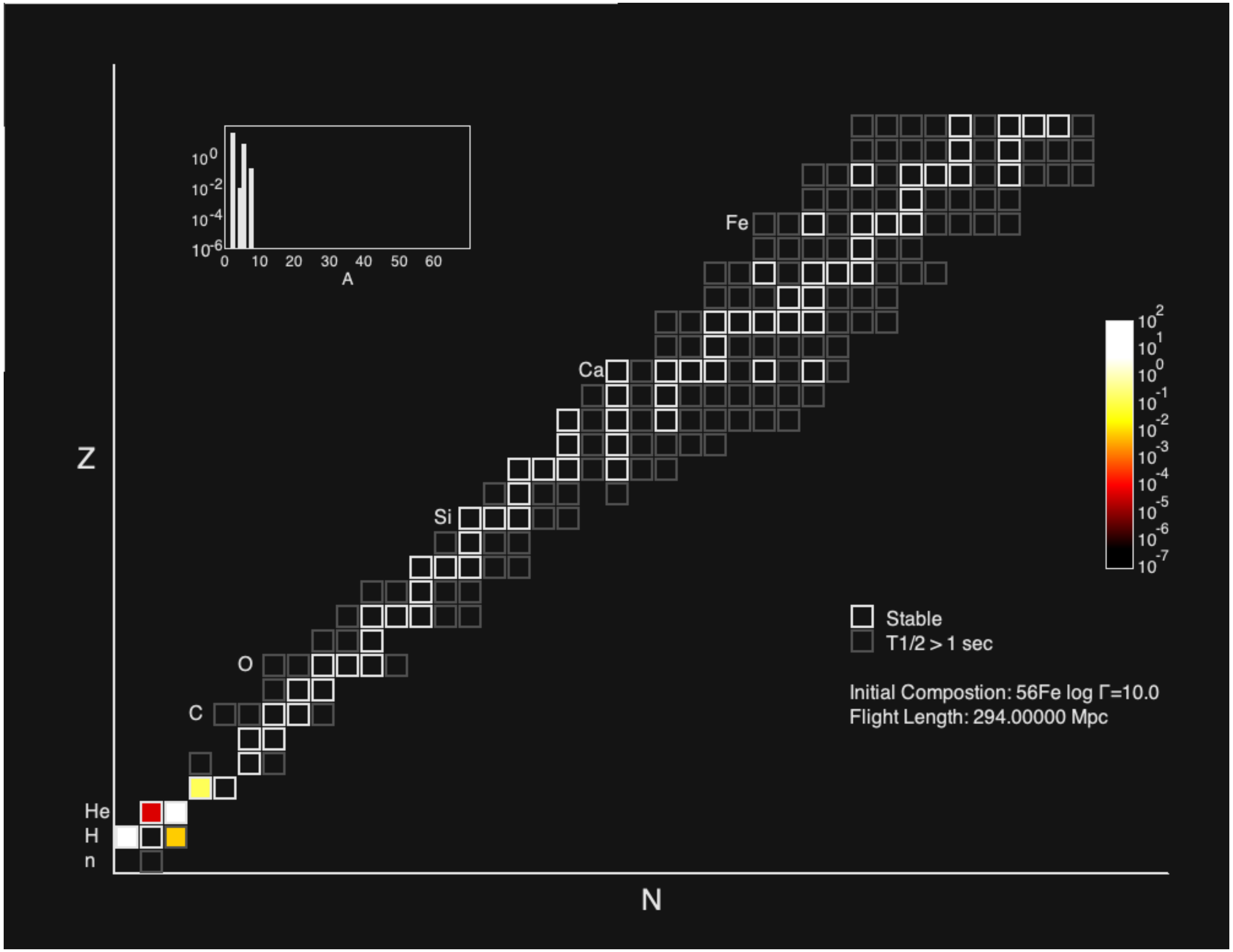

UHECR: Intergalactic Propagation by a Toy-Model Simulation

500 Mpc

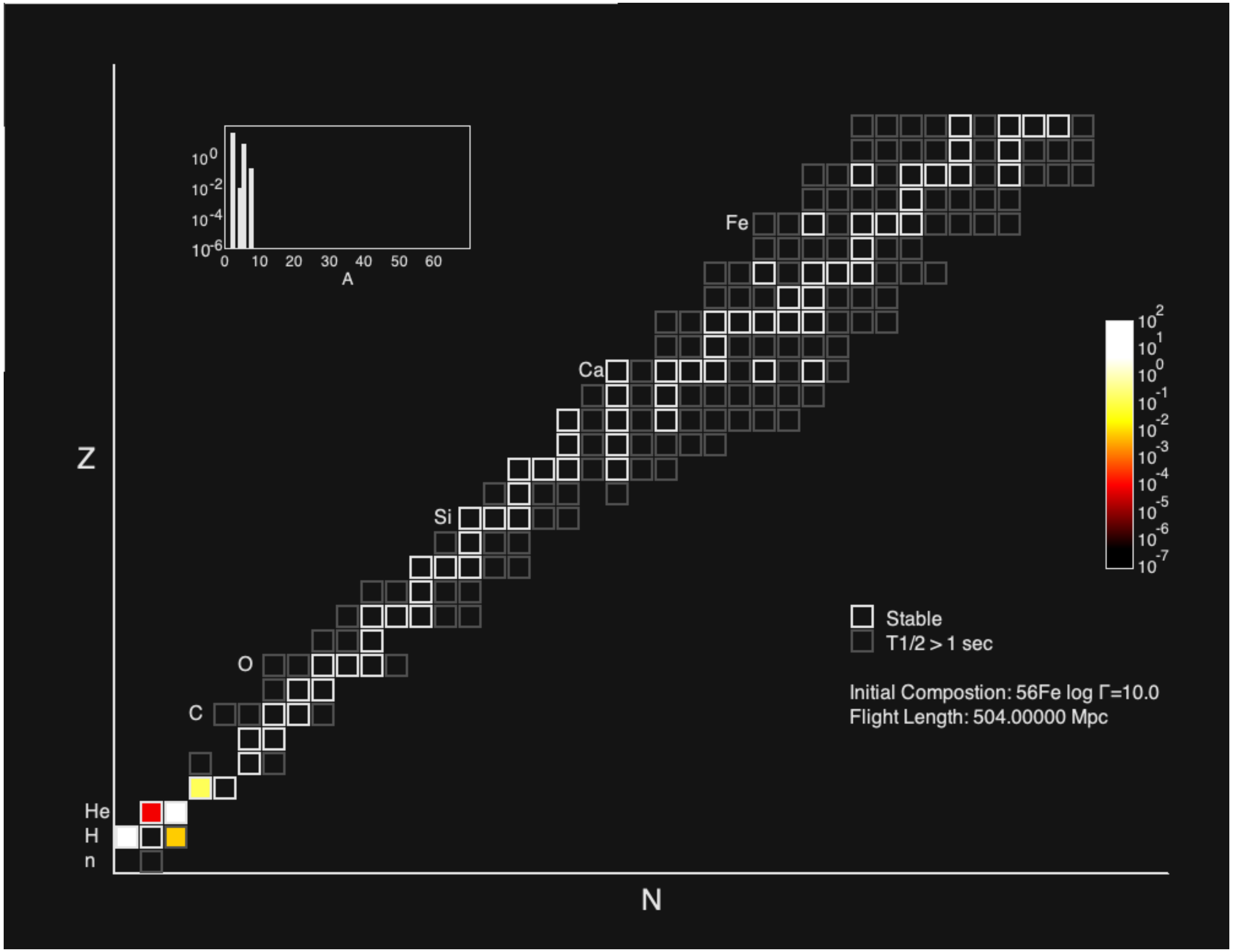

Experimental Methods

Probing Photo-Nuclear Response of Nuclei

Virtual photo excitation by proton scattering (RCNP, iThemba LABS)

- Missing mass method
  with proton Coulomb excitation

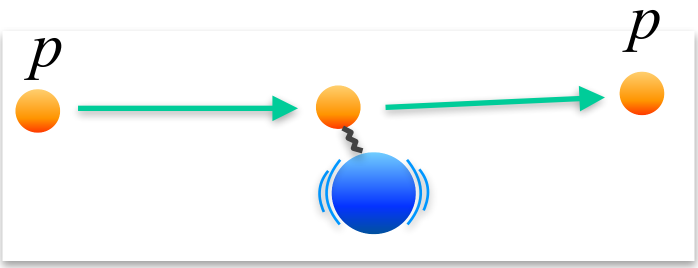

- better for total strength
  and strength distribution
  higher cross sections
  also applicable for p,α,γ decays

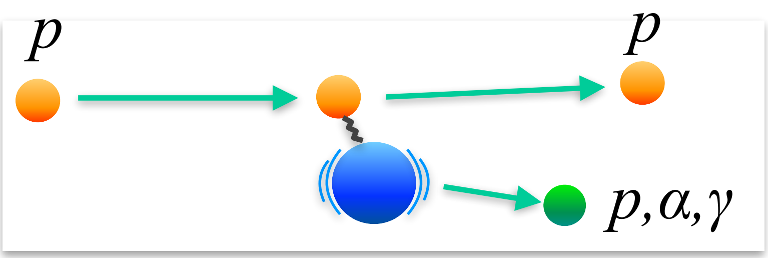

Real photo excitation (ELI-NP etc.)

- Gamma-beam by laser-Compton
  scattering with an electron beam

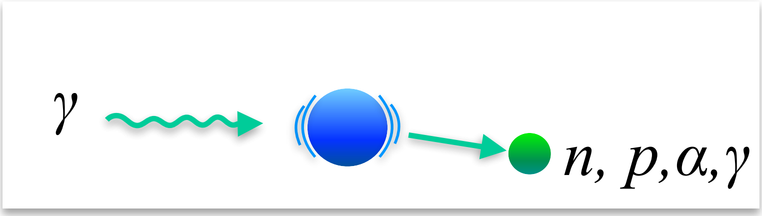

- individual decay channels
  better for absolute normalization
  applicable also for *n* and *xn* decays in addition to p,α,γ

Research Center for Nuclear Physics, The University of Osaka

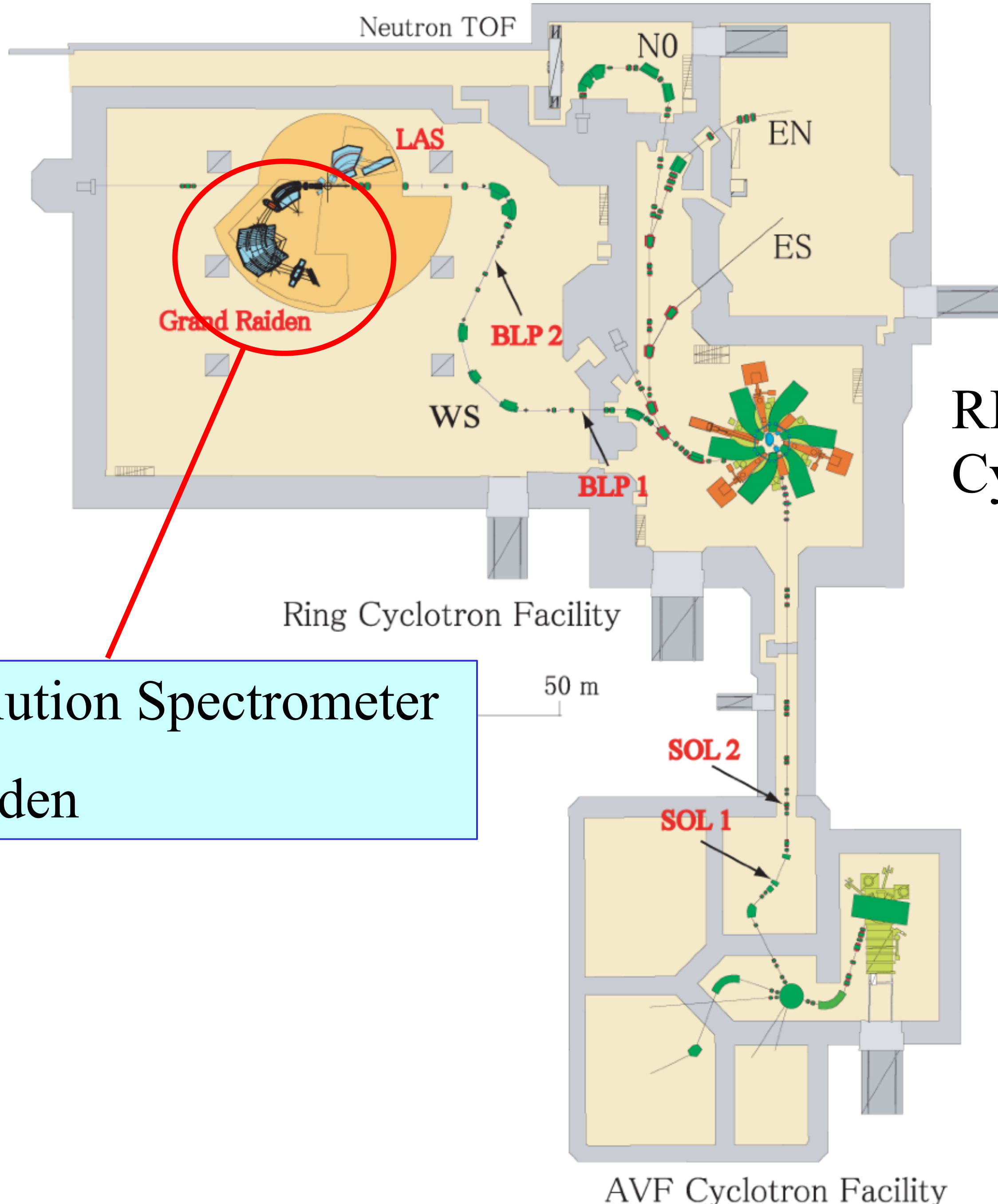

a proton beam at 392 MeV

RING Cyclotron

Injector AVF Cyclotron

High-resolution Spectrometer

Grand Raiden

High-Resolution Spectrometer "Grand Raiden"

Proton scattering
at very forward angles

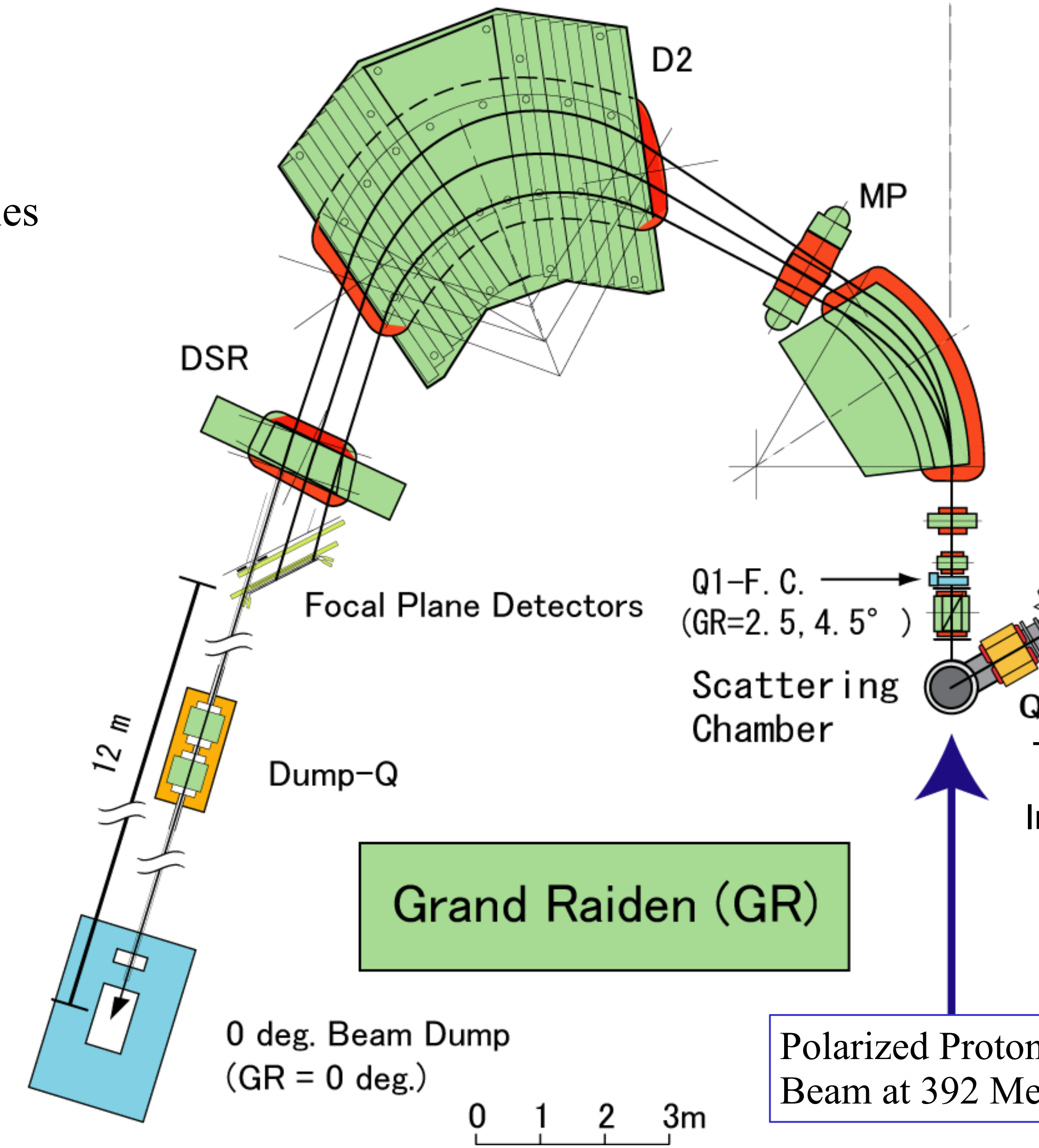

Target: 1 (10) mg/cm²

Intensity : 1-8 nA

Polarized Proton
Beam at 392 MeV

Virtual photo excitation by proton scattering

- Missing mass measurement with Coulomb excitation
- coincidence for p,α,γ branching ratio

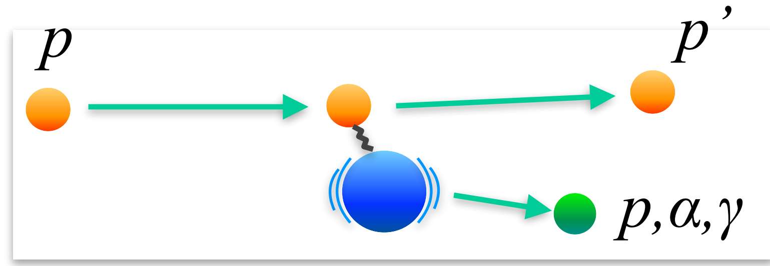

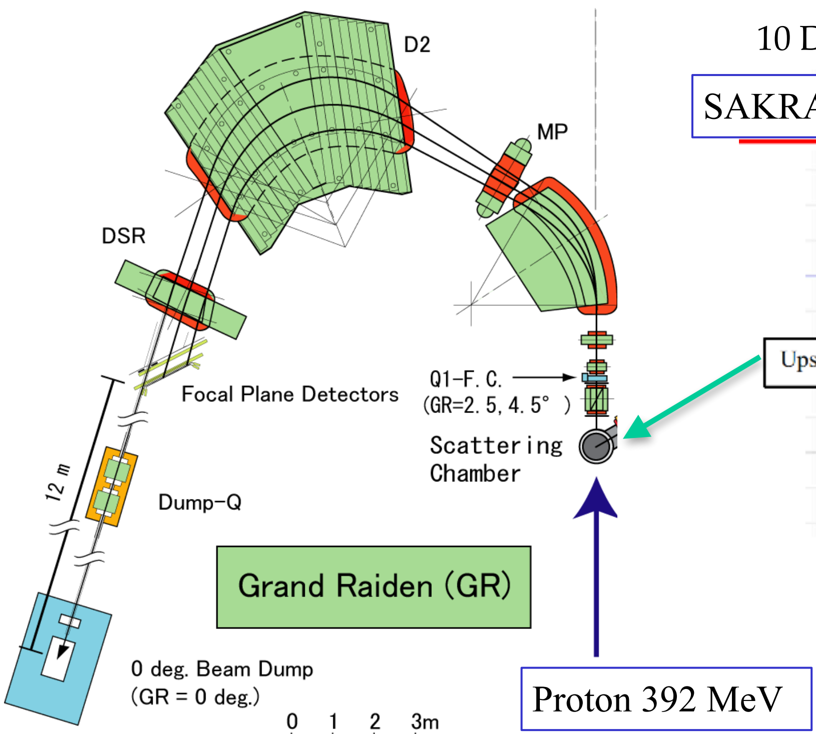

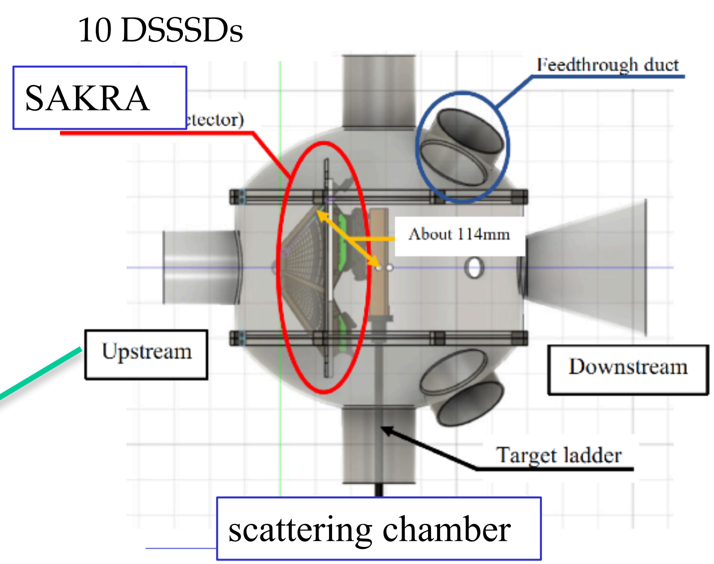

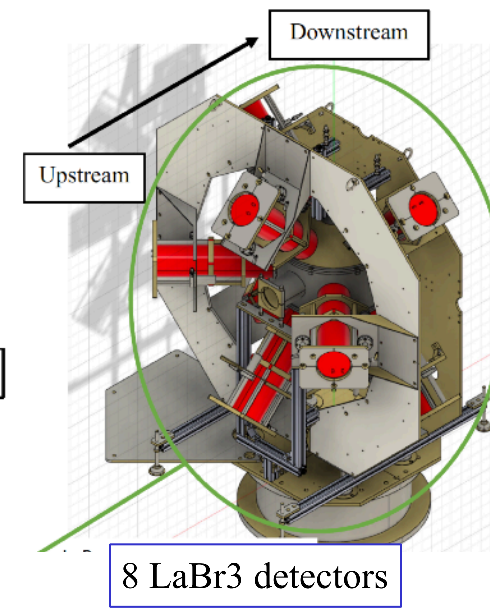

3.5″ϕ-8″L

E536: 1st PANDORA experiment at RCNP, Oct. 2023



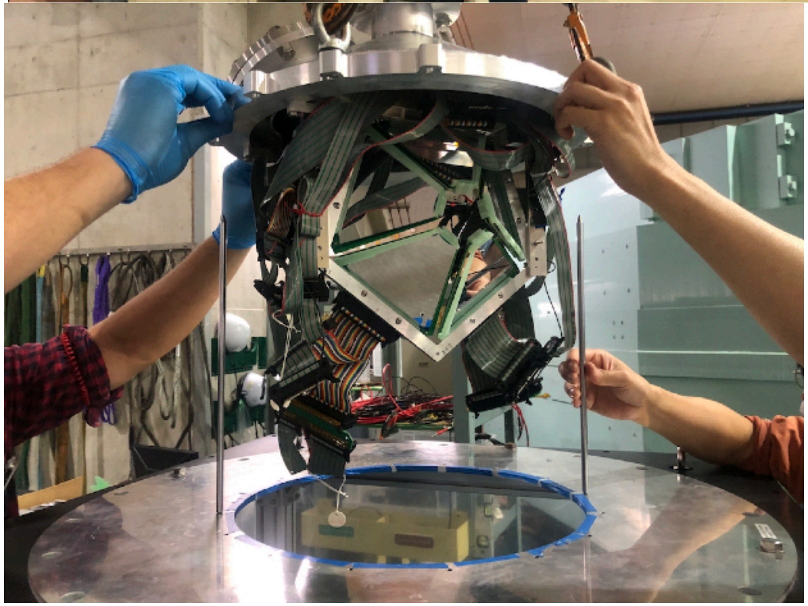
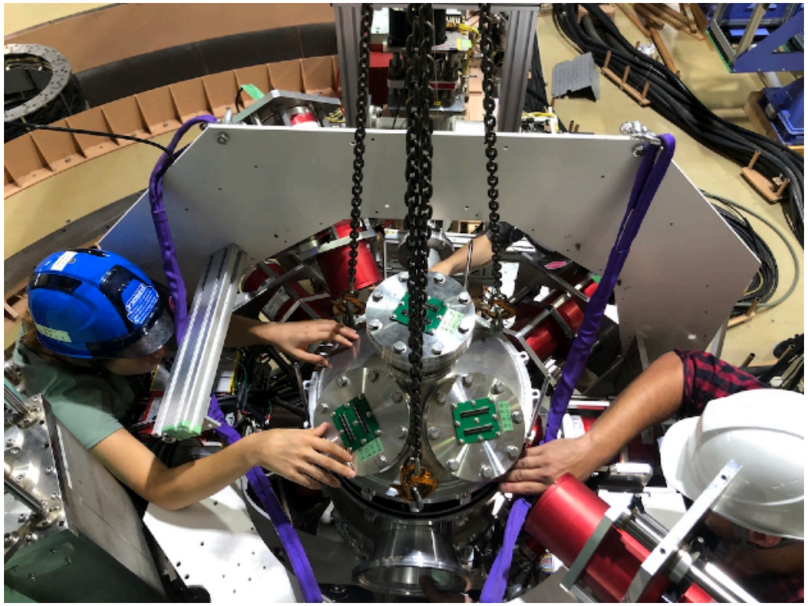

E589: 2nd PANDORA experiment at RCNP, Oct. 2025

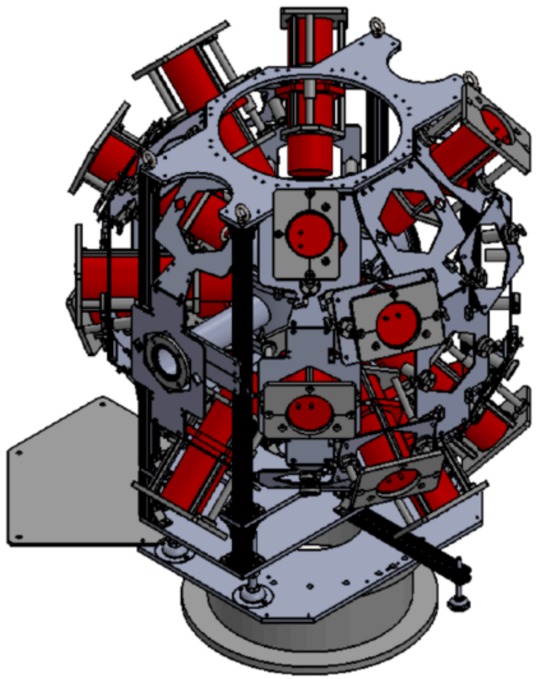

LPIS: 16 large volume LaBr3 detectors

8 from Milano

8 from iThemba LABS

LaBr3 detectors from iThemba LABS

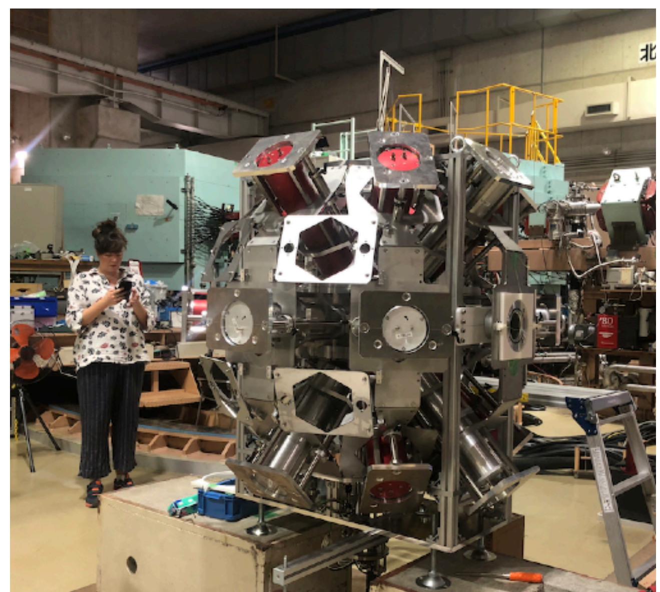

LPIS: LaBr3 detectors mounted

red: Milano

紅

white: iThemba LABS

白

Targets

Measurements on 10-20 nuclei
with theoretical model developments

σ_{abs} distribution and decay
branching ratios in 10% accuracy

Candidate target nuclides

• ^{12}C, ^{16}O and ^{27}Al	first cases, alpha decay, reference target
• ^{6}Li, ^{7}Li, ^{9}Be, ^{10}B, ^{11}B	light nuclei
• (^{20}Ne), ^{24}Mg, ^{28}Si, ^{32}S, (^{36}Ar), ^{40}Ca	N=Z nuclei, α-cluster effect, deformation
• ^{26}Mg, ^{48}Ca, ^{56}Fe	N>Z nuclei
• ^{13}C, ^{14}N, ^{51}V	odd and odd-odd nuclei
• (γ,xn) on ^{18}O, ^{48}Ca, ^{64}Ni	

Measured in 2023 thin box & 2025 thick box

- [red box] photo-abs. c.s. + charged particle decay + gamma
- [teal box] photo-abs. c.s. + gamma

^{27}Al photoabsorption and charged particle decay

analyzed by Y. Sasagawa 

^{27}Al photo-reaction: available data

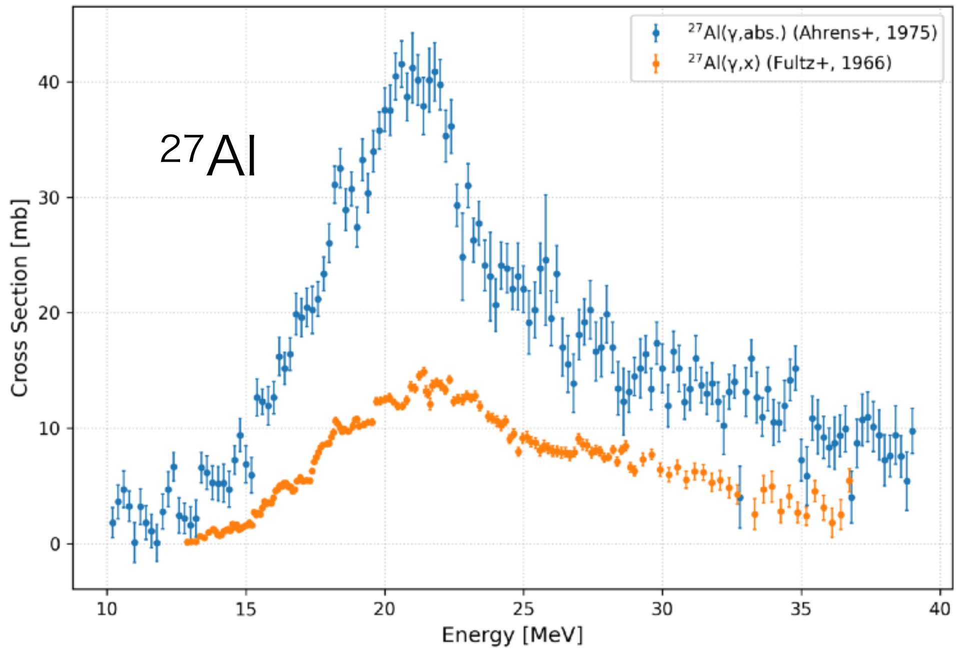

← (γ, abs)

← $(\gamma, n) + (\gamma, 2n)$ Fultz et al., L0039

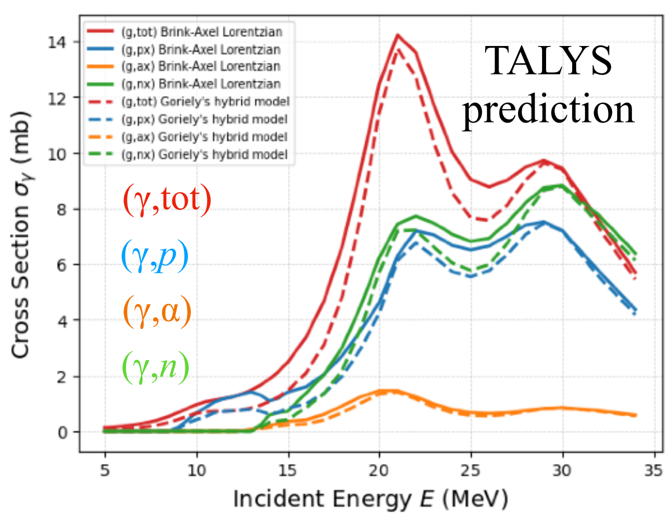

The peak photo-absorption cross section is significantly underestimated .(~ 1/3)

$^{27}Al(p,p')$ Differential Cross Section

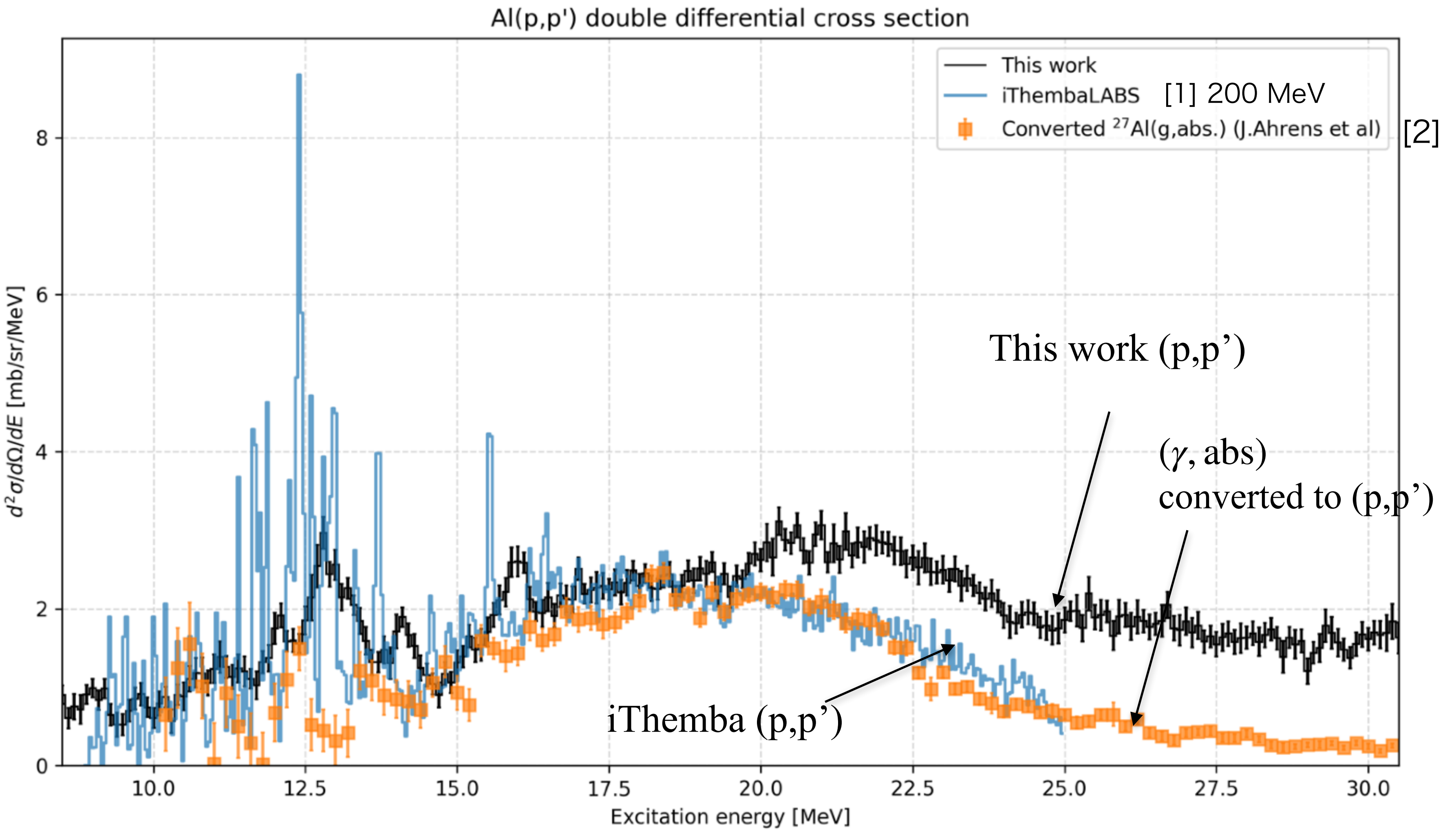

[1] M. Jingo *et al*., Eur. Phys. J. A 54, 224 (2018).

[2] J. Ahrens *et al*., Nucler Phys. A 251, 479(1975).

Charged Particle Decay Coincidence

(MeV)	proton	deuteron	alpha	neutron
^{27}Al	8.3	17.1	10.1	13.1

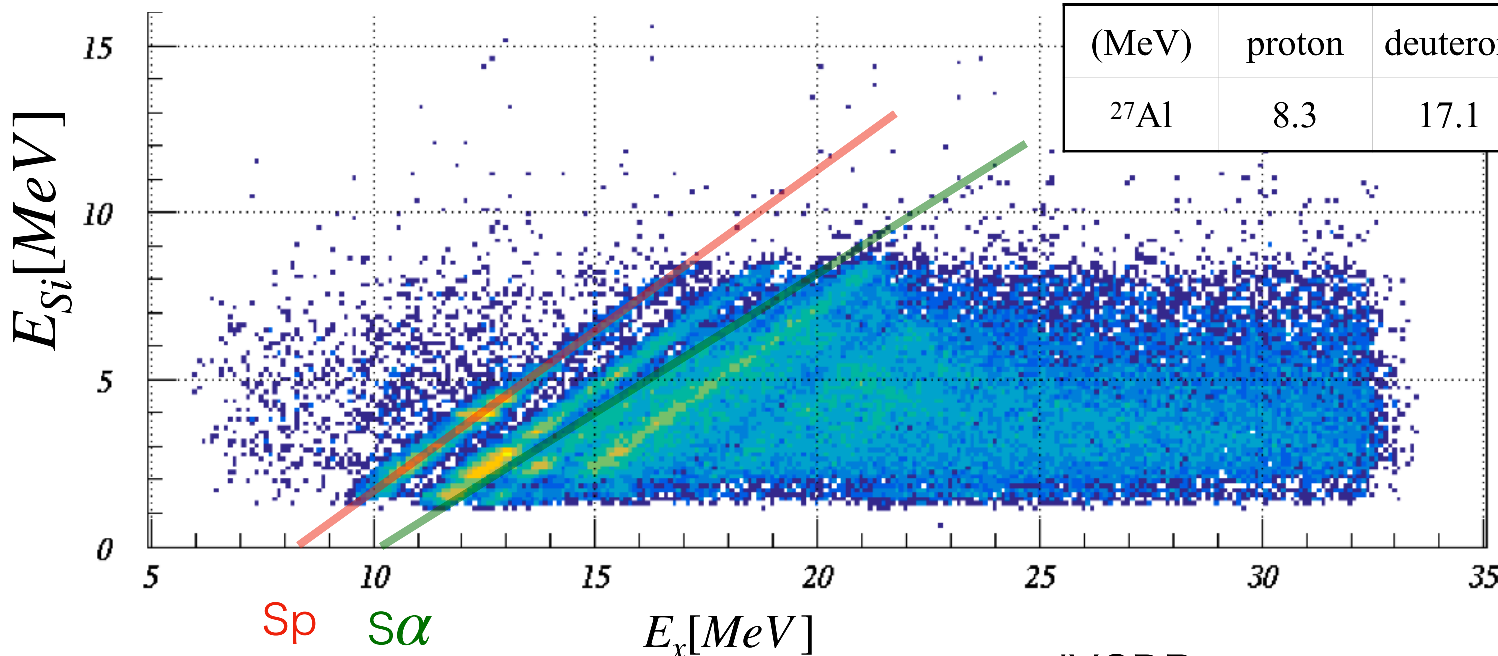

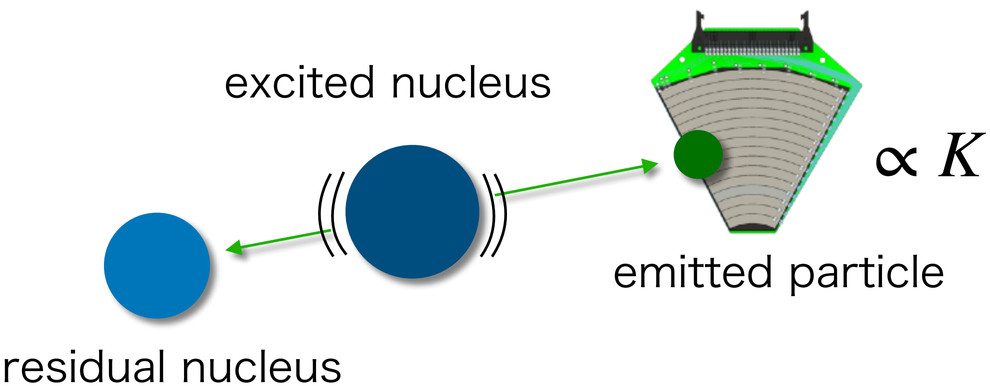

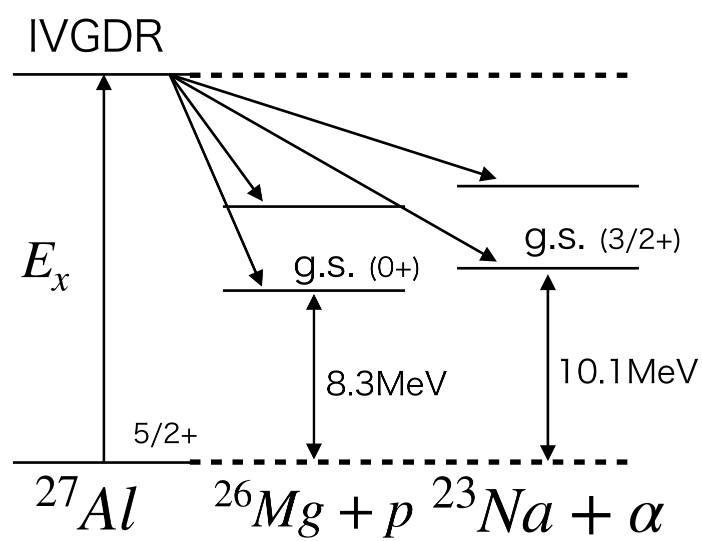

$$E_x(target) \rightarrow S\ (+E_x(residual)) + K$$

Charged Particle Decay Coincidence

(MeV)	proton	deuteron	alpha	neutron
^{27}Al	8.3	17.1	10.1	13.1

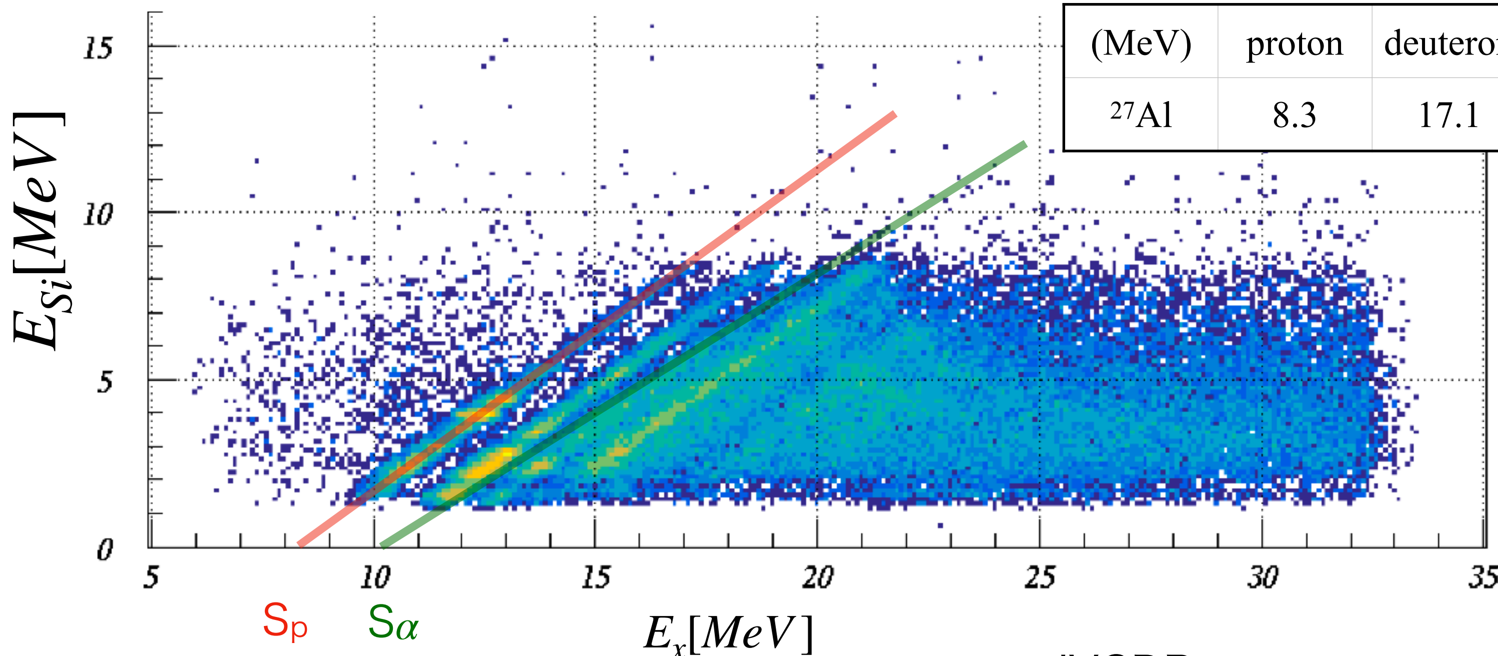

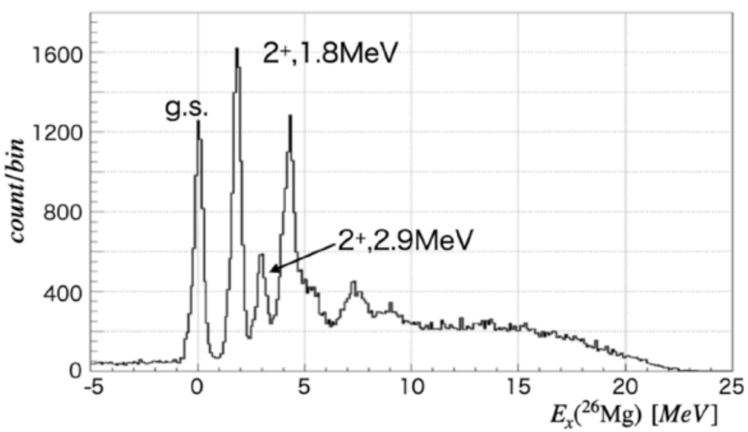

daughter states assuming proton-decay

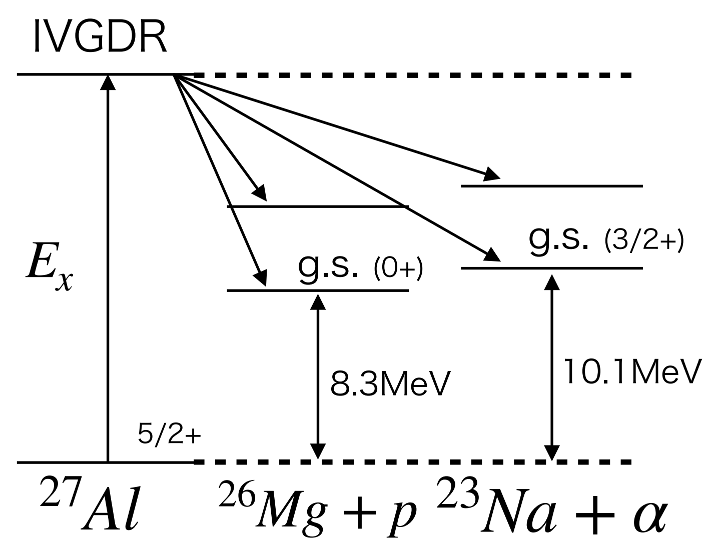

Preliminary Results

Differential Cross Section at 0 degrees

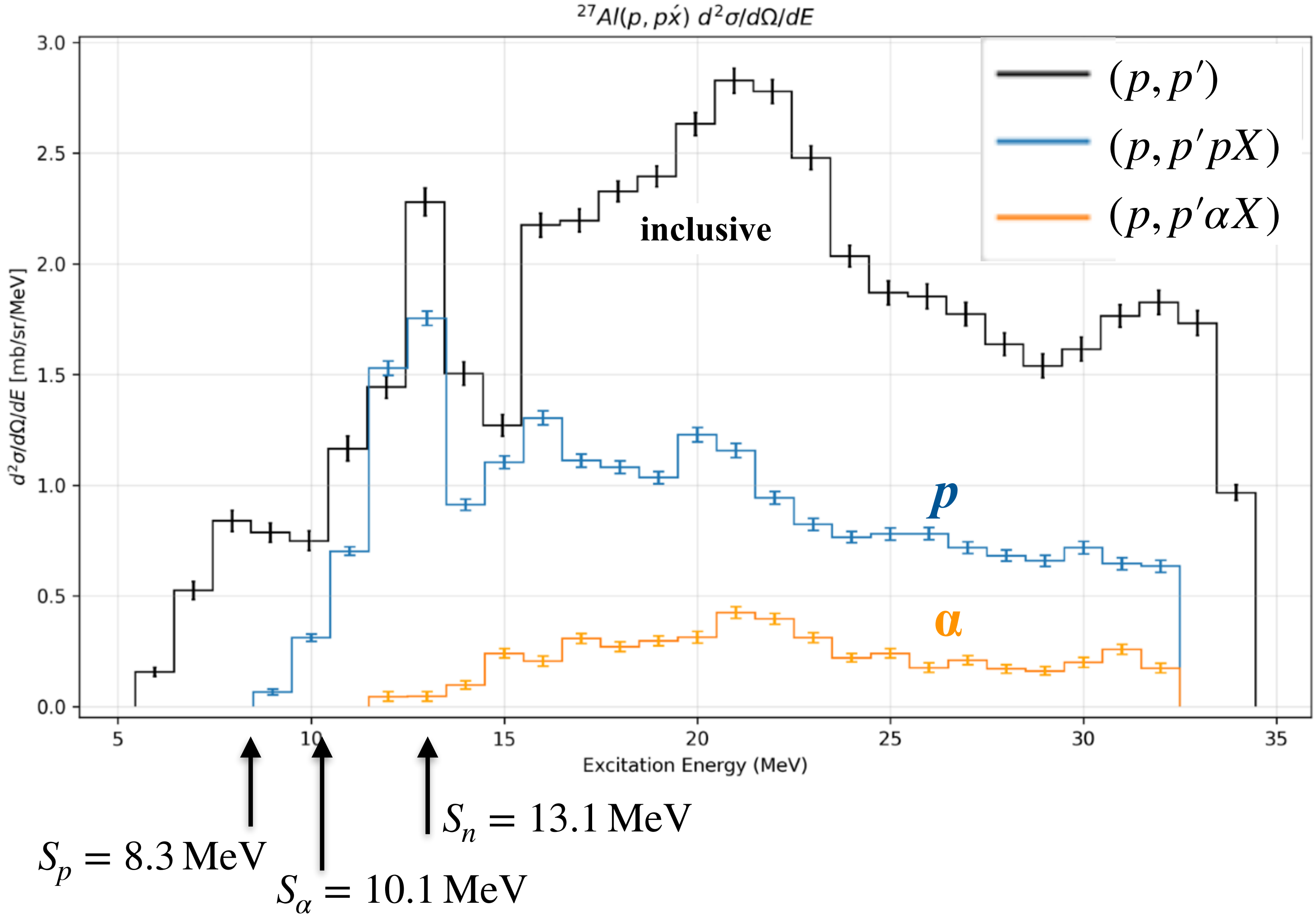

Decay Branching Ratios

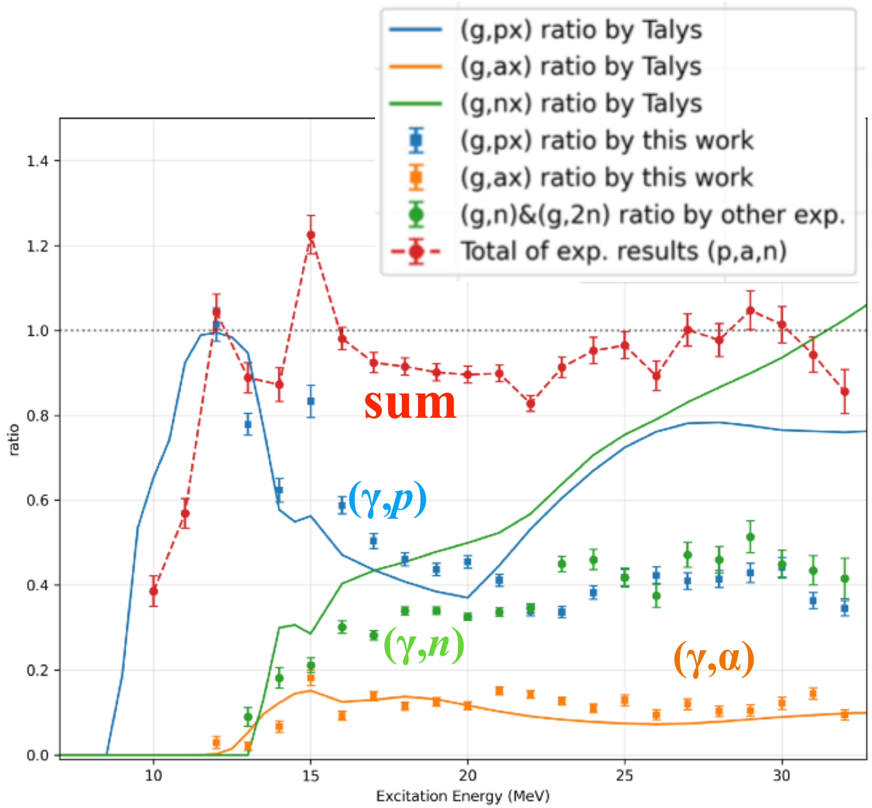

Statistical Errors are shown for this work

TALYS prediction

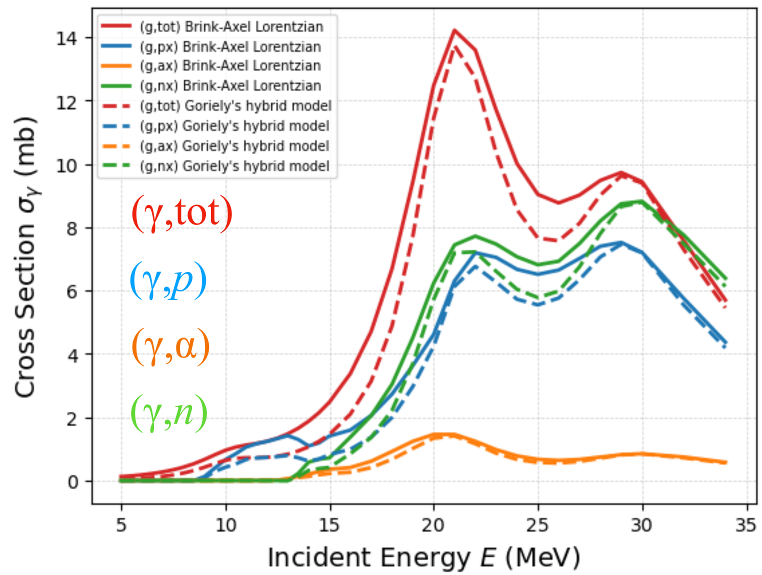

photo-reaction cross sections

separation energies

	α	p	n	d	αp	αn	pp	nn	pn
^{27}Al	10.1	8.3	13.1	17.1	18.9	22.5	22.4	24.4	19.4

Multi-particle decays are not treated properly yet.

n and p branching ratios:

comparable above 20 MeV

α decay: ~10% above 15 MeV

Well predicted by TALY

Summary

- Photo-absorption cross sections and decay branching ratios of light stable nuclei are systematically studied up to A~60 in the PANDORA project.
- The photo-nuclear reaction data are important for developing nuclear structure/decay models and for simulating the inter-galactic propagation of UHECRs.
- Virtual photon excitation by proton scattering has been applied at RCNP.
- Preliminary data on ^{27}Al has been shown.

Thank you for your attention

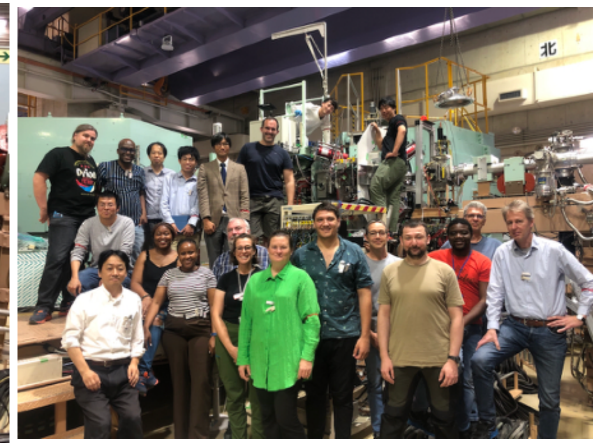

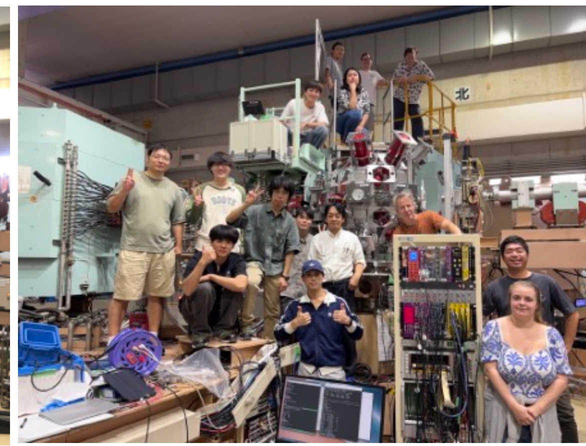

Thank you, all the collaborators!

PANDORA

Photo-Absorption of Nuclei and Decay Observation for Reactions in Astrophysics

※ Not all the collaborators are shown in the pictures.

Backup Slides

Historical Methods

Bremsstrahlung Beam + Activation Analysis

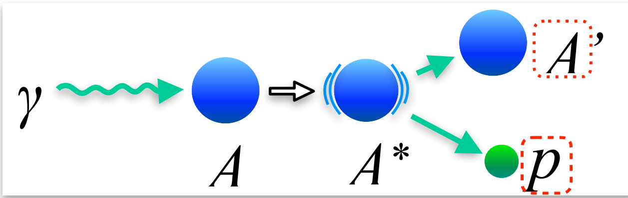

- High-intensity gamma-rays
- Continuous photon spectrum with decreasing intensity at higher energy requires
  - taking difference with different beam energy

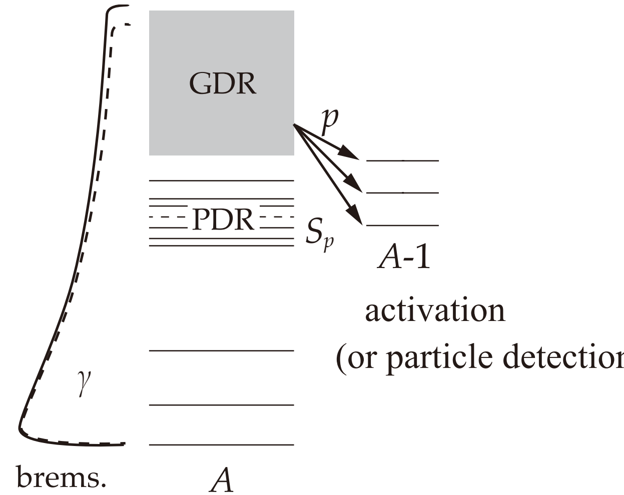

Positron Annihilation in Flight

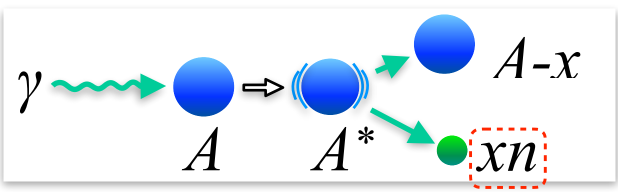

- Energy resolution (≥500 keV)
- Limited beam intensity
- Systematic difference between Livermore and Saclay data (non-flat neutron detection efficiency?)

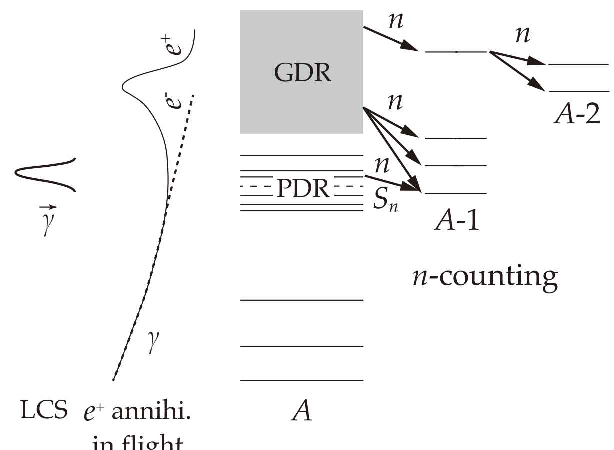

(γ, n), (γ, xn)

T. Kawano et al., NDS163_109 (2020)

Real Photon Beams: Continuous Energy

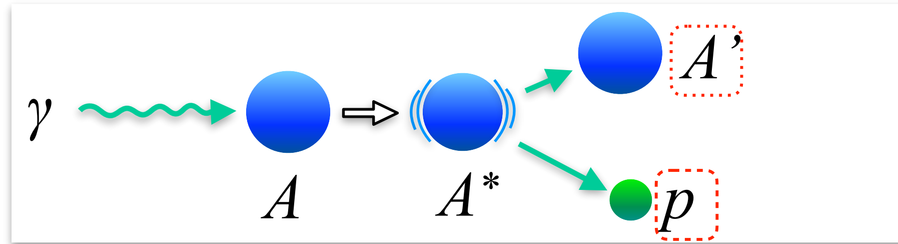

I. Real photon beams

1.Continuous energy beams

a. Bremsstrahlung

- High-intensity gamma-rays
- Continuous photon spectrum with decreasing intensity at higher energy requires
  - taking difference with different beam energy
  - precise knowledge on the photon spectrum is required for precise measurement on photo-nuclear reaction cross sections in GDR region.

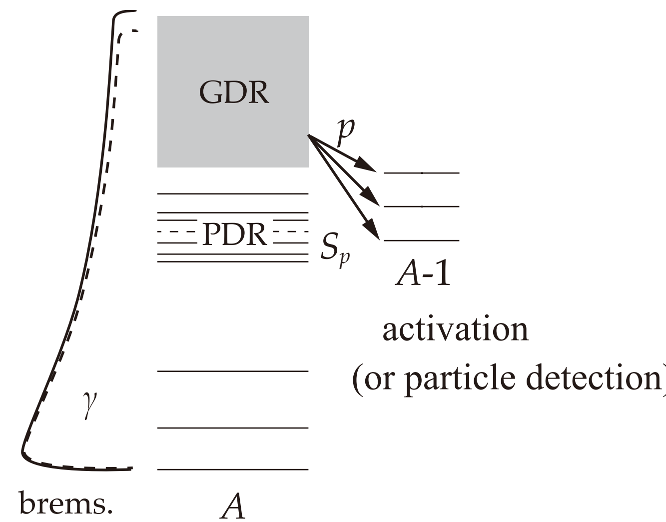

Monoenergetic or quasi-monoenergetic photon beams are essential for reliable measurements in the continuum (GDR) region.

Real Photon Beams: Quasi-Monoenergetic

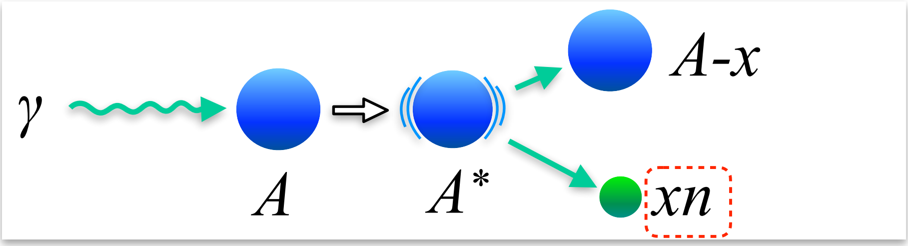

I. Real photon beams

2. Quasi-monoenergetic beams

Positron Annihilation in Flight

Lawrence Livermore, Saclay

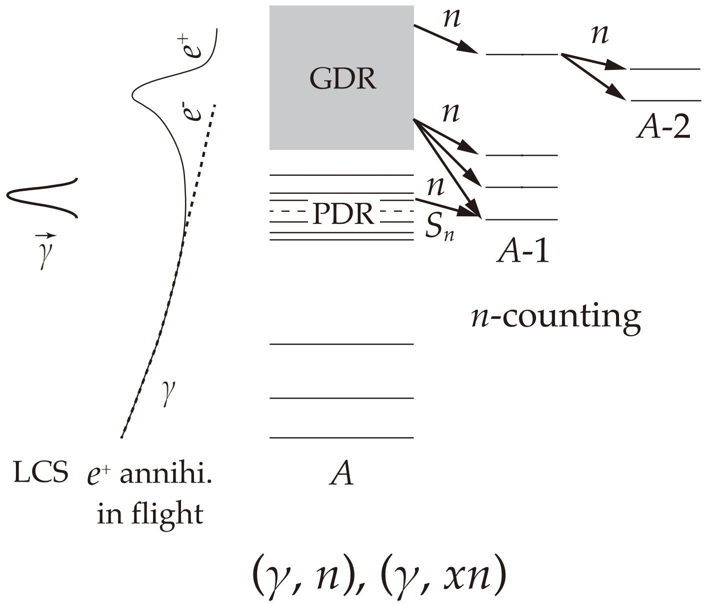

- Energy resolution (≥500 keV)
- Limited beam intensity: inapplicable to thin targets for isotopically enriched or for charged-particle decays.
- Inconsistency between Livermore and Saclay (γ,xn) data T. Kawano et al., NDS163_109 (2020)

UHECR: Anisotropy

[anc19]

Auger and TA

Small directional variation of flux is observe in almost isotropic distribution:

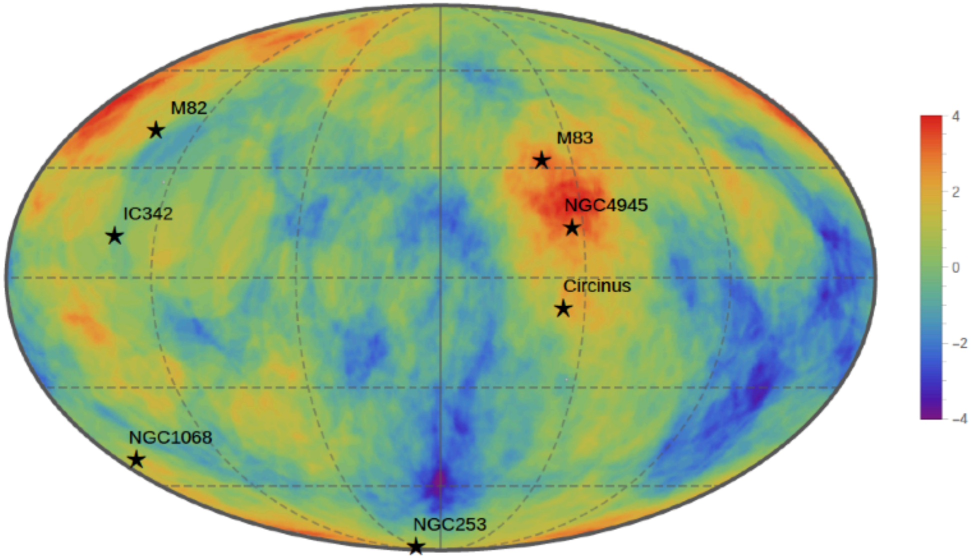

Candidate production sites

Active Galactic Nuclei

Starburst Galaxies

Figure 7: Skymap in Galactic coordinates of the Li-Ma significances of over-densities in 20° radius windows for 840 events recorded by Auger with $E > E_{\mathrm{th,Auger}}$ and 130 events recorded by TA with $E > E_{\mathrm{th,TA}}$. The color scale indicates the significance in units of standard deviations; negative values follow the convention of indicating the (positive) significance of deficits. Nearby SBGs providing a significant contribution to the UHECR correlation signal of Auger [3] and TA [163] are indicated by stars. From Ref. [161].

Auger data with a model prediction of deflection of UHECRs by galactic and extragalactic magnetic fields.

Magnetic Rigidity ∝ E/Z

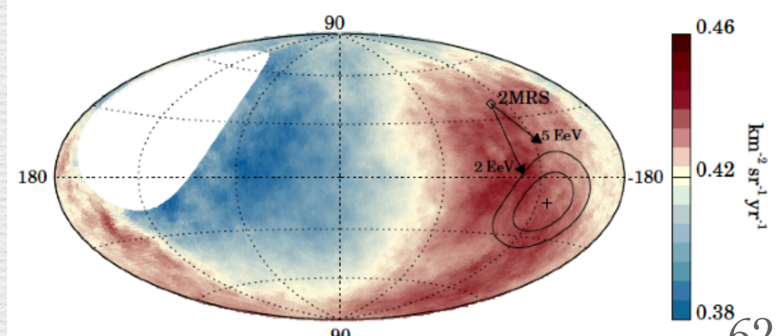

Measurement of the Photo-Nuclear Reaction and decay branching ratios by proton scattering

Virtual photo-excitation by proton scattering at forward angles

- Missing mass method with proton Coulomb excitation
- applicable for p,α,γ decays

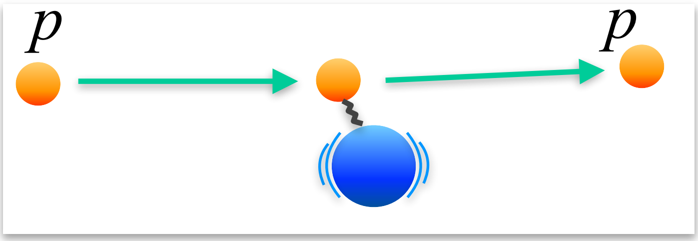

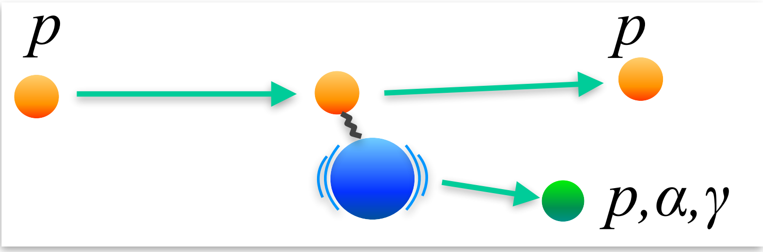

Multipole-decomposition analysis of the angular distribution to extract *E1*.

P. von Neumann-Cosel and AT, EJPA'19

AT et al., NIMA'09

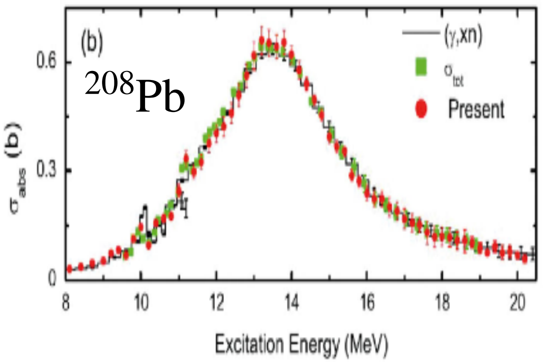

AT et al., PRL'11

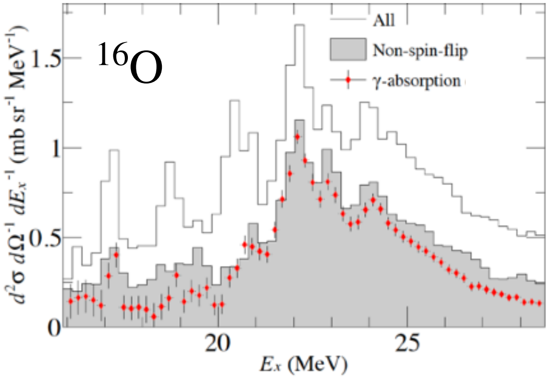

T. Sudo et al., RCNP-E398

UHECR spectrum after their extragalactic propagation

Assuming :
(i) a uniform distribution of extragalactic sources
(ii) standard candle sources emitting a power law spectrum of UHECRs (i.e $N(E) \sim E^{-\beta}$)

A set of parameters which allows a satisfactory reproduction of the UHECR spectrum and composition are (for the code used in Allard et al., 2005) :

(i) a source spectral index β=0.61
(ii) a low maximum energy at the sources $E_{max}(Z)$=Zx4.10^{18}eV where Z is the charge of the nucleus
(iii) relative abundances : H=0.1, He=0.15, CNO=0.68, Si=0.07, Fe=0.002 (NB : no astrophysical motivations)

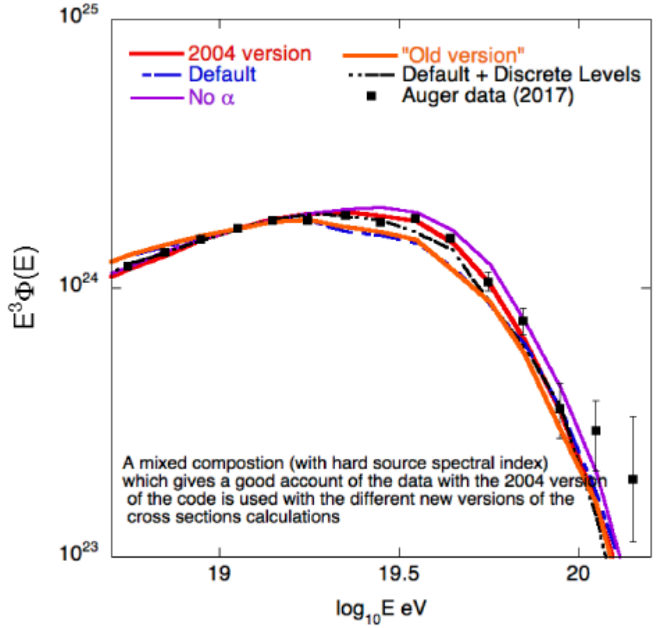

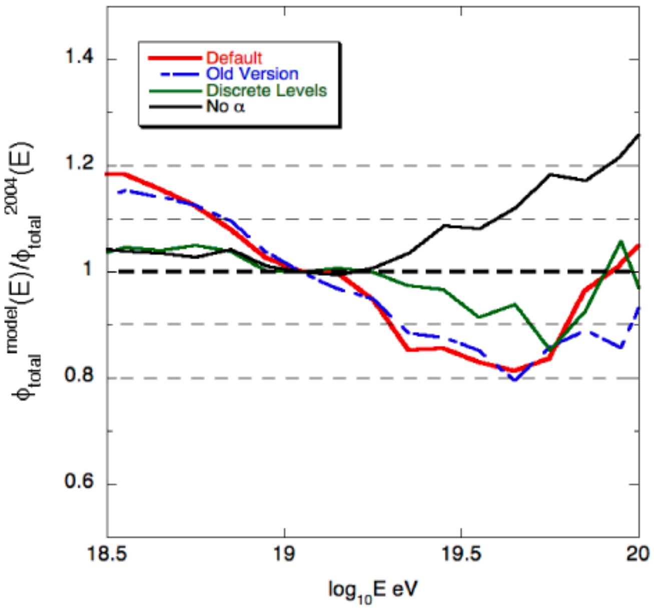

* The spectrum with the "No α" settings is quite harder than the other —> slower photodisintegration
* "Discrete Levels" settings and the 2004 version are quite close to each other
* The "default" and "old settings" are softer

Why is that so ?

—> channels involving α particles in light nuclei (e.g,(γ,α), (γ,n+α), …), see next slides

Comparison of the simulated spectral shape

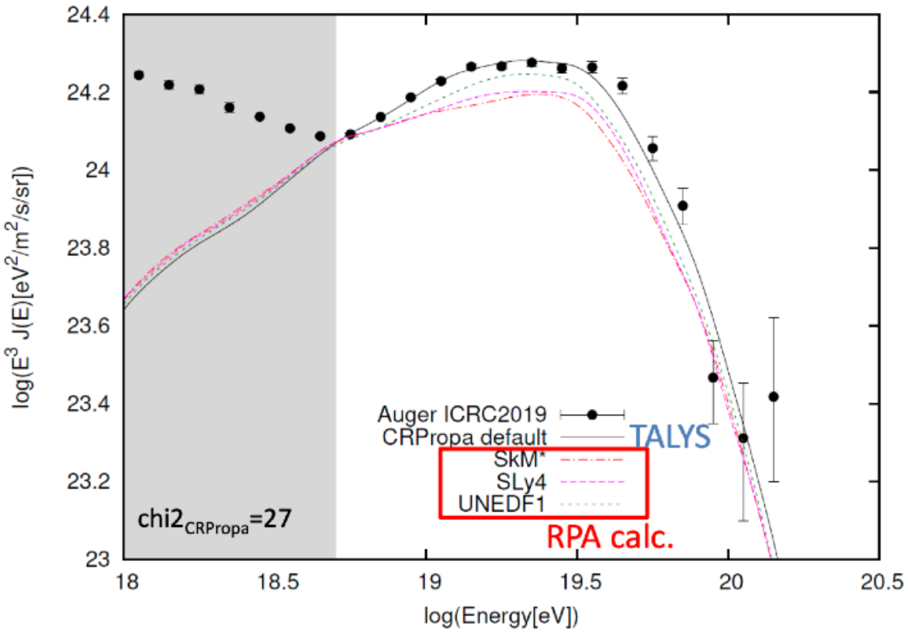

The RPA implies lower cutoff rigidity than TALYS mainly because of the difference in the GDR peaks. This is the opposite effect to the PSB model.

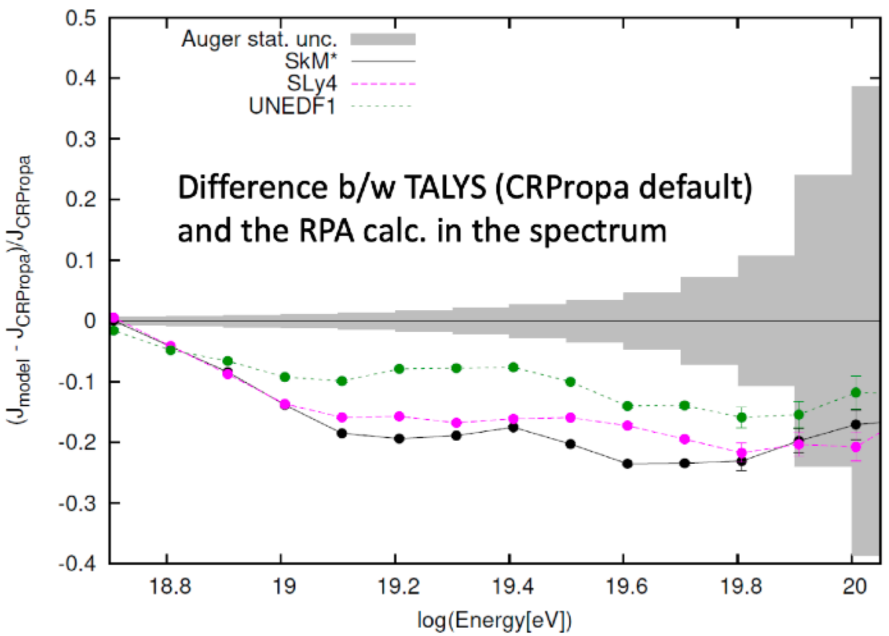

The difference: more than the statistical uncertainty of the experimental data.

E. Kido et al., Astropart. Phys. 2023

Energy Loss Process of UHECRs in Extragalactic Propagation

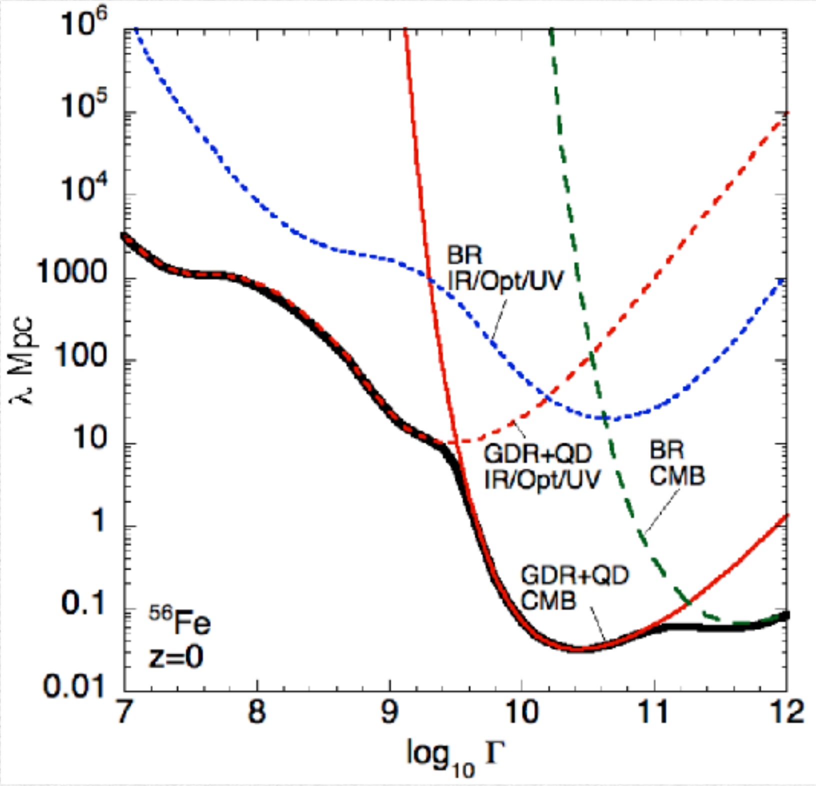

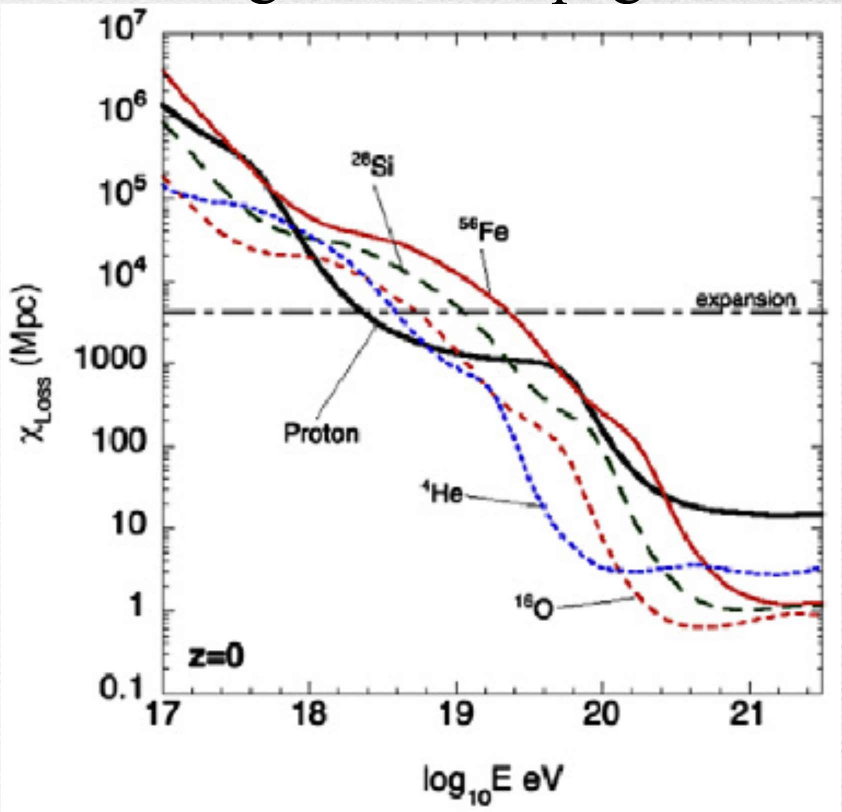

Refinements of the theoretical model in [kha05]

[ste99]

Unfortunately, photodisintegration cross section data are incomplete. For many reaction channels, $\sigma(\epsilon)$ data do not exist. Also, integrated cross section strengths are not available for all of the exclusive channels. The most complete compilation of the world's GDR cross section data exists in the 15 volumes of Fuller & Gerstenberg (1983). In these volumes GDR cross section data for ^{56}Fe, for example, are given only for the (γ, pX) channel and the inverse channels (α, γ) and (p, γ).